# The effects of type II Golgi-localized proton pyrophosphatase *AVP2;1/VHP2;1* mutations on cell wall and root growth under low boron condition in *Arabidopsis thaliana*

シロイヌナズナのタイプ II ゴルジ体局在プロトンピロホスファターゼ *AVP2;1/VHP2;1* 遺伝子変異の低濃度ホウ素条件における細胞壁と根の成長に対する影響

**ONUH, AMARACHUKWU FAITH**

**Division of Biosphere Science,**

**Graduate School of Environmental Science,**

**Hokkaido University**

**2023**

# Contents

This work has been partly published in the paper referenced below:

Onuh, A. F., and Miwa, K. (2023). Mutations in type II Golgi-localized proton pyrophosphatase *AVP2;1/VHP2;1* affect pectic polysaccharide rhamnogalacturonan-II and alter root growth under low boron condition in *Arabidopsis thaliana*. *Front. Plant Sci*. 14. 1255486. doi.10.3389/fpls.2023.1255486

**Abstract**

Plants generally require mineral nutrients for growth and development. One of the mineral nutrients required by plants is boron. Boron, though a trace nutrient because it is required in a little amount, is essential for plant growth. Its deficiency symptoms have been observed in many plants and it is widely spread across the globe. Some approaches to combat low boron stress such as fertilizer application and upregulation of boron transporters have been exploited. The approach of fertilizer application is mostly limited by its potential environmental pollution when washed out of the soil. Another limitation is the difficulty in ascertaining the optimum required fertilizer amount because of the wide range of boron requirement among plant species. The approach of upregulation of boron transporters, although useful for the reduction of boron fertilizer application, does not provide a lasting solution to boron deficiency. The implication of the upregulation of boron transporters is an increase in boron uptake which will eventually lead to a depletion of the limited soil boron in the long term. Knowing the down sides of the approaches to boron deficiency thus far, there is the need for a better system. The major role of boron known so far is the stabilization of the plant cell wall. The pectin component of the primary cell wall is composed of three major polysaccharides homogalacturonan (HG), rhamnogalacturonan I (RG-I) and rhamnogalacturonan II (RG-II). RG-II exists in the cell wall as a dimer and this dimerization/crosslinking of the RG-II monomers is by boron. The synthesis of the pectic polysaccharides takes place in the Golgi apparatus, acidified by proton pumps. AVP2;1/VHP2;1 is a type II proton pyrophosphatase localized in the Golgi apparatus, which possesses proton pumping activity coupled with pyrophosphate hydrolysis. Its activity and expression patterns have been previously revealed but its role in plants remains unknown. In the screening of mutants which could grow under low boron condition, a mutant carrying a missense mutation in *AVP2;1* was

isolated. The aim of the present thesis therefore was to explore the physiological role of AVP2;1 in *Arabidopsis thaliana*.

The isolated mutant carrying a missense mutation in *AVP2;1* showed increased primary root growth under low boron conditions but no significant difference under normal boron condition compared to wild type plants. T-DNA insertion mutants in *AVP2;1* showed similar phenotype of enhanced root growth under low boron. The quantification of mRNA level of *AVP2;1* in *avp2;1* mutants and wildtype Col-0 confirmed that T-DNA insertion mutants were knock down mutants suggesting that reduced function of AVP2;1 was responsible for the improved root growth. All the mutants also showed an improved root growth under low boron condition in hydroponic culture system (a more natural system), consistent with the growth tests conducted in solid media. Under low pH and low phosphorus conditions, *avp2;1* mutants showed no obvious difference in growth compared to the wildtype, suggesting that the increased roots by *AVP2;1* mutation were specific to low boron. For a better understanding of what could possibly have impacted the improved root growth of mutants under low boron condition, root cells of the plant lines were microscopically observed. The root cell observation by microscopy revealed an increase in meristematic zone length, the cell number in meristem and length of matured cell in *avp2;1* mutants compared to wildtype under low boron condition. To explore the possible mechanism behind the increased root growth under low boron in *avp2;1* mutants compared to wildtype, the hypothesis of changes in cell wall components was considered because of the role of boron in cell wall stability. Analysis of the root cell wall components revealed that calcium concentration was reduced in mutant root cell wall under low boron condition. RG-II specific sugars also tended to be decreased in mutant root cell wall under low and normal boron conditions, suggesting reduction in RG-II synthesis and boron binding capacity in cell wall in the mutants. The implication of the reduction of RG-II in mutants is that the amount of boron required for crosslinking of RG-II would be reduced and hence the improved root growth of mutants under

low boron supply. To support this, previous research has shown that there is a positive correlation between cell wall boron concentration and RG-II amount among different plant species. This implies pectin amount or RG-II amount determines sensitivity to boron deficiency hence the reduced sensitivity to low boron in *avp2;1* mutants.

Taken together, the results obtained from this study suggest that changes in cell wall component by mutations in *AVP2;1* may possibly explain the increased root length of *avp2;1* mutants under low boron by the mechanism of reduced boron requirement. This study supports the idea that AVP2;1 plays a role in proton pumping and acidification of Golgi apparatus for maintenance of pectin synthesis by examination of *avp2;1* mutants. It also proposes the idea of a reduction of boron requirement by molecular approach as a sustainable strategy against low boron stress rather than fertilizer application and upregulation of boron transporters.

**List of abbreviations**

| | |
|---|---|
| aa | amino acid |
| AIR | alcohol-insoluble residue |
| B | boron |
| bp | base pair |
| Ca | calcium |
| cDNA | complementary DNA |
| Col-0 | Columbia-0 |
| d | days |
| DNase | deoxyribonuclease |
| EMS | ethyl methanesulfonate |
| HG | homogalacturonan |
| ICP-MS | inductively coupled plasma-mass spectrometry |
| min | minute(s) |
| mRNA | messenger ribonucleic acid |
| PCR | polymerase chain reaction |
| PI | propidium iodide |

| | |
|---|---|
| RG-I | rhamnogalacturonan I |
| RG-II | rhamnogalacturonan II |
| rpm | revolution per minute |
| sec | second(s) |
| U | unit(s) |
| v | volume |
| WT | wildtype |

# 1 Introduction

Mineral nutrients are essential for plant growth and development. By the use of these mineral nutrients, plants are able to synthesize organic compounds such as carbohydrates and amino acids needed for their proper growth. Depending on the amount required for proper growth, the mineral nutrients are divided into major and minor/trace nutrients. The major nutrients are required in a high quantity and examples of such nutrients are nitrogen, phosphorus, potassium, calcium etc. The minor/trace nutrients on the other hand, are required in little amount and examples are boron, zinc, copper etc.

Boron (B) is one of the plant micronutrients. Boron exists in the soil as boric acid or borate and is taken up primarily as boric acid (Miwa and Fujiwara, 2010). This makes boron the only mineral nutrient taken up not as an ion but as an uncharged molecule. It is conisdered to have a very high permeablility across lipid bilayers and as a result, transportation of boron into the plant cells was thought to be only by passive diffusion (Raven, 1980). However, nowadays it has been revealed that transportation of boric acid into the cell is majorly via special boron transporter proteins especially under low boron conditions. According to (Dannel et al., 2002), transportation of boron via passive diffusion only occurs when the concentration of boron is high, whereas in a limited supply of boron, transportation of boron via facilitated transport is initiated. Therefore, in addition to passive diffusion, the presence of channel-mediated facilitated diffusion and energy-dependent active transport against concentration gradients in boron transport systems have become the recognized mechanism for boric acid transport (Dannel et al., 2002). Two types of boron transporters have been identified through molecular and genetic approach in *A thaliana* and in other plant species; the nodulin 26-like intrinsic proteins (NIPs) which are channel proteins and borate transporters (BOR) which are high-affinity active transport proteins (Miwa and Fujiwara, 2010; Takano et al., 2008). Under low boron conditions, the channel proteins NIP5;1 imports

boric acid from the soil into the epidermal, cortical and endodermal cells and the borate transport protein BOR1, exports boric acid/borate from the endodermis into the xylem (Takano et al., 2008). The regulation of these boron transporters contributes to modulating the boron amount in the plant cells.

As a result of the fact that boron exists in the soil as boric acid, it is easily leached under high rainfall conditions leading to boron deficiency (lack of enough boron in plants). Due to this fact, boron deficiency is seen to be prevalent in areas with high amount of rainfall (Shorrocks, 1997; Yan et al., 2006). Boron deficiency is one of the vast spread micronutrient deficiencies around the world, causing great quantitative and qualitative losses in crop production. It has been reported in more than 80 countries and for 132 crops over the last 60 years (Shorrocks, 1997). Depending on the plant age and species, the severity of boron deficiency is diverse and some of the boron deficiency symptoms include inhibition of leave expansion, root growth and fertility. A limited supply of boron has been found to impair cell enlargement and cell division in the meristematic zones hence the inhibition of root growth and leaf expansion under low boron supply. Seeing the adverse effect of boron deficiency on both quantitative and qualitive yield of plants, there is therefore a great need for its mitigation. Various mitigatory approaches such as management of nutrient condition by fertilizer application have been explored. The application of borate fertilizers to make up for the insufficient soil boron is limited by its cost and effectiveness (Güneş et al., 2003; Duran et al., 2018; Fujiyama et al., 2019). Its ineffectiveness is due to the difficulty to ascertain the optimum required fertilizer amount because of the wide range of boron requirement among plant species (Gupta et al., 1985). There is a narrow window between boron deficiency and toxicity and hence inappropriate application of borate fertilizer may lead to toxicity. On the other hand, the use of molecular approach as a mitigatory measure for boron deficiency has been exploited. This involves the overexpression of the boron transporters BOR1, BOR2 and NIP5;1 in plant species like *Brassica napus, Zea mays, Arabidopsis thaliana, Oryza sativa* etc. to

improve boron deficiency tolerance (Onuh and Miwa, 2021). Though this approach is useful for the reduction of boron fertilizer application, it still does not completely solve the problem of low-boron stress. This is because upregulating these boron transporters would increase boron uptake thereby leading to a depletion of the limited soil boron in long term. Hence, there is a need for a better measure to mitigate low-boron stress.

The plant cell wall is a structural layer of the cell which provides protection, strength, and rigidity to the cell and therefore to the plant. A fully developed cell wall is a complex structure of three distinct layers, the middle lamella, the primary cell wall, and the secondary cell wall. The primary cell wall is composed of cellulose, hemicellulose, pectin, and soluble proteins. Its major component is pectin making up 30-50% of the primary cell wall (Cosgrove and Jarvis, 2012). The pectin component is structurally heterogenous, consisting of three different types of polysaccharide domains: homogalacturonan (HG), rhamnogalacturonan-I (RG-I) and rhamnogalacturonan-II (RG-II) (Mohnen, 2008; Alba and Kontogiorgos, 2017). Minerals such as calcium (Ca) and boron (B) in the pectin, are essential for the crosslinking of HG and RG-II, respectively, which forms the pectin network and aids the overall stability of the primary cell wall. RG-II has HG as a backbone and six distinct side chains A-F (Ndeh et al., 2017; Voxeur et al., 2017) and it has been experimentally demonstrated that RG-II exists as a dimer crosslinked by a borate diester in the plant cell wall (Kobayashi et al., 1996). The major function of boron discovered and experimentally shown so far is its stability of the primary cell wall by crosslinking of RG-II (Matoh et al., 1993; O'Neill et al., 2001).

The pectic polysaccharides of the plant cell wall are synthesized in the Golgi apparatus by the activity of Golgi-localized proteins (Driouich et al., 1993; Lerouxel et al., 2006) and subsequently transported through the TGN (trans-Golgi network) in an acidic condition. With the use of pH sensors, estimated pH was 6.8 and 6.3 in cis-Golgi and TGN in *A. thaliana* protoplasts, respectively (Shen et al., 2013), and it was 6.3 and 5.6 in trans-Golgi and TGN/EE (early

endosome) in *A. thaliana* root cells, respectively (Luo et al., 2015). The presence of two types of proton pumps in the Golgi apparatus and TGN which are possibly responsible for its acidification and ion homeostasis has been established in plants. These proton pumps are the vacuolar type ATPase (V-ATPase) (Luo et al., 2015) and proton pyrophosphatase ($H^+$-PPase). The $H^+$-PPase has a dual function of hydrolysis of pyrophosphate (PPi) into two ortho-phosphates in the cytosol and proton pumping into the Golgi apparatus. The energy generated from the hydrolysis of PPi by this enzyme is what powers its translocation of proton into the Golgi apparatus.

Generally, two types of $H^+$-PPase, the type I and type II exist in plants (Drozdowicz et al., 2000). From 27 plant species, 124 $H^+$-PPase members have been identified using complete genomic data and 123 members belonged to type I or type II (Zhang et al., 2020). In *A. thaliana*, there are three genes which encode $H^+$-PPase. Type I is encoded by *AVP1/VHP1/FUGU5* (At1g15690) and type II by *AVP2;1/VHP2;1* (At1g78920) and *AVP2;2/VHP2;2* (At1g16780). AVP2;1 and AVP1 share 33% amino acid sequence identity whereas AVP2;1 and AVP2;2 share 94% amino acid sequence identity (Segami et al., 2010). The AVP2s, which have a $Mg^{2+}$-binding motif, have been reported to have an obligatory requirement for $Mg^{2+}$ and an insensitivity to potassium ions ($K^+$) for their PPi hydrolytic enzymatic activities (Drozdowicz et al., 2000). According to Segami et al., (2010), AVP2s also show characteristics of $Zn^{2+}$ dependency for its enzymatic activity. Segami et al. (2010) have revealed that the AVP1 and the AVP2s whose protein levels are less than 0.3% of AVP1, are localized to the tonoplast (AVP1) and the Golgi apparatus and TGN (AVP2s). So far it has also been found that AVP1 is abundant in shoot apical meristem, leaf primordia and pollen in *A. thaliana* while AVP2s are abundant in young roots, buds, flowers and siliques (Segami et al., 2010, 2014). The functional characterization of AVP1 in *A. thaliana* has been established by studies in mutants and overexpression lines. Some of its known roles are regulation of auxin-mediated organ development and involvement in various abiotic stress tolerance (Li et al., 2005; Kim et al., 2014; Nepal et al., 2020; Zhang et al., 2023).

It has also been shown that rather than proton pumping, PPi hydrolysis activity is the major contribution of AVP1 in organ development as demonstrated using *fugu5* mutants (Ferjani et al., 2011; Asaoka et al., 2016). However, little is known about the AVP2s and their mutant phenotype.

In this study, AVP2;1 was focused and from the screening of *A. thaliana* mutants with enhanced root growth under low boron, a mutant carrying a missense mutation in *AVP2;1* was isolated. T-DNA lines of *AVP2;1* showed similar root growth suggesting that the reduced function of AVP2;1 was responsible for the phenotype. Here the phenotypic unveiling of *avp2;1* mutants and the possible effect of *AVP2;1* mutation on cell wall synthesis are reported. These findings give insight into the possible function(s) of AVP2;1 in plants with regards to boron nutrition and propose a possible novel mitigatory measure for low boron stress.

## 2 Materials and methods

### 2.1 Plant materials and growth conditions

Columbia-0 (Col-0), an ecotype of *Arabidopsis thaliana* (L.) Heynh was used as wildtype (WT) in this study. The mutant number 31A hereafter referred to as *avp2;1-4/ vhp2;1-4* used in this study was obtained via the screening of Col-0 seeds mutagenized with ethyl methanesulfonate (EMS) (Hiroguchi et al., 2021). This screening was performed under severe boron deficient (0.03 µM) condition and the mutant showed longer root than Col-0 under this condition and no difference from Col-0 under normal (100 µM) boron condition. This mutant carries a base substitution of guanine to adenine (G800A in CDS and G2492A in full length genomic sequence from the transcriptional start site) which caused an amino acid substitution (G267D in protein). *AVP2;1* (At1g78920) T-DNA insertion mutants SALK_0542912 in Col-0 background (Alonso et al., 2003)and SAIL_165F07 in Col-3 background (Sessions et al., 2002) hereafter referred to as *avp2;1-2/ vhp2;1-2* and *avp2;1-3/ vhp2;1-3*, respectively, were also used. T-DNA insertion position for both lines is the $6^{th}$ intron of At1g78920. These T-DNA insertion mutants were obtained from the Arabidopsis Biological Resource Center (ABRC). To determine homozygosity of T-DNA insertion, PCR was performed using the sets of primers listed in Table 1.

Seeds were surface sterilized using a washing solution containing 30 mL tap water, 3 mL of bleach (5-10% hypochlorous acid) and 3 drops of detergent, rinsed five times with sterilized ultra-pure water, suspended in ultra-pure water and stored in the dark at 4°C for 4 days before being sown. Plants were cultured in solidified MGRL media (Fujiwara et al., 1992) in which boron concentration was adjusted with boric acid. Growth conditions of 0.06 µM and 0.1 µM boric acid for low boron condition, 0.2 µM, 0.3 µM and 1 µM boric acid for mildly low boron condition, 100 µM boric acid for normal boron condition and 3000 µM boric acid for toxic boron condition were set. The MGRL solid media contained 1% (w/v) sucrose and 1% (w/v) gellan gum (Wako

Pure Chemicals). Plants were incubated in a vertical position at 22°C under a 16-hour light/8-hour dark cycle.

For fertility test, surface sterilized seeds were first grown in ultra-pure water on rockwools for 7 days. Seedlings were transferred to liquid MGRL media supplemented with 0.1 µM, 0.3 µM, 0.5 µM and 100 µM boric acid and incubated for 49 days making it a 56-day growth period. The incubation condition for both growth in ultra-pure water and liquid culture was set at 22°C under a 16-hour light/8-hour dark cycle (long day) and a relative humidity of 70%. Liquid culture was changed weekly during the initial 14 days after transfer, and subsequently changed twice in a week.

### 2.2 Plant materials and growth condition under other stresses

Surface sterilized wildtype Col-0 and *avp2;1* mutants were used. For low phosphorus treatment, plants were grown in half strength Murashige and Skoog (MS) solidified media containing 3.5 mM MES and pH adjusted to 5.68 using KOH. The phosphorus concentration was adjusted with $KH_2PO_4$. Growth conditions of 12.5 µM phosphate for low phosphorus condition and 625 µM phosphate for normal phosphorus condition were set. The MS media also contained 1% (w/v) sucrose and 1% (w/v) agar (for plant culture medium, Wako Pure Chemicals with catalogue number of 010-15815). For the pH test, half strength of MS solidified media solution was prepared containing 3.5 mM MES. pH was set as 4.29 (low pH) with HCl and as 5.7 (normal pH) with KOH. The solid media also contained 1% (w/v) sucrose and 1% (w/v) agar (for plant culture medium, Wako Pure Chemicals with catalogue number of 010-15815). Plants were incubated in vertical positions at 22°C under a 16-hour light/8-hour dark cycle until analysis.

## 2.3 Genotyping of T-DNA insertion mutants of *avp1* and *avp2;2* mutants and growth conditions

To determine homozygosity of T-DNA insertion mutants, DNA was extracted from shoots of 7-d-old T-DNA lines (*avp1* and *avp2;2*) and wildtype Col-0 seedlings grown under 100 µM boron condition. PCR was performed on *avp1* mutant GABI_596C07 (Yang et al., 2018) represented as *avp1-4* and *avp2;2* mutants SALK_044701 (*avp2;2-1*) and SALK_138132 (*avp2;2-2*) (Tojo et al., 2023) using the primers listed in Table 1. For growth analysis, plants were cultured in solidified MGRL media in which boron concentration was adjusted with boric acid. Growth conditions of 0.06 µM and 0.1 µM boric acid was set for low boron conditions while 100 µM boric acid was set for normal boron condition. The MGRL solid media contained 1% (w/v) sucrose and 1% (w/v) gellan gum (Wako Pure Chemicals). Plants were incubated in a vertical position at 22°C under a 16-hour light/8-hour dark cycle.

## 2.4 Quantitative reverse-transcription PCR (qRT-PCR)

Surface-sterilized seeds of Col-0 and *avp2;1* mutants were sown in solid medium containing different concentrations of boric acid for 9 days. Roots were harvested and immediately frozen using liquid nitrogen for RNA extraction. The frozen samples were homogenized at 1700 rpm for 15 sec four times using Multi beads shocker (YASUI KIKAI) in a 3 mL tube. Total RNA was extracted using RNeasy Plant Mini Kit (Qiagen, Germany) and treated with RNase-free DNase (Qiagen, Germany) for 30 mins to eliminate genomic DNA contamination. cDNA was synthesized from 0.25 µg total RNA using the PrimeScript RT reagent kit (TAKARA). Expression level of *AVP2;1*, *NIP5;1*, *BOR1*, and *BOR2* was analyzed by qRT-PCR using Thermal Cycle Dice (TAKARA, Japan) with SYBR premix Ex Taq II (TAKARA, Japan). The mRNA level of *AVP2;1* was detected at the 5' (upstream) portion and 3' (downstream) portion of T-DNA insertion. *EF1α*

was used as a reference gene for normalization of the target mRNA level. For the conversion of Ct to the relative amount of cDNA, a standard curve was first made with a dilution series of cDNA. The standard curve showed a plot of measured Ct values (number of cycles by second derivative maximum method) against the log of known concentrations of templates. By the measured Ct of unknown samples, initial template amounts were then calculated from the standard curve. Primers used are listed in Table 1.

### 2.5 Measurement of primary root length

For the measurement of primary root length, photographs of 9-day-old seedlings grown under 0.06 µM, 0.1 µM, 0.2 µM, 0.3 µM, 100 µM and 3000 µM boric acid were taken and the digital image was analyzed using an imaging processing software, ImageJ.

### 2.6 Observation of primary root under stereomicroscopy

Surfaced sterilized seeds of Col-0 and *avp2;1* mutants were grown under 0.1 µM boric acid (low boron), 0.3 µM boric acid (mildly low boron) and 100 µM boric acid (normal boron) in solid media for 5 days. Root tips of plant lines were observed and photographed using a stereomicroscope (OLYMPUS SZX12) equipped with a moticam1080 (Shimadzu).

### 2.7 Measurement of root cell length and number

Col-0 and *avp2;1-4* mutant were grown under low boron (0.1 µM) and normal boron (100 µM) in MGRL solid media for 5 days. The plant roots were stained with 10 $mgL^{-1}$ propidium iodide (PI: FUJIFILM Wako Pure Chemical, Japan). The imaging data was obtained using a LSM980 (Zeiss, Germany) confocal laser scanning microscope at an excitation and emission wavelength of 543 nm and 543 nm-694 nm. The obtained images were exported with the Carl Zeiss ZEN 3 blue edition software. The length of fully elongated cortical cells and root apical meristem (RAM)

length were measured using ImageJ software. The fully elongated cortical cells or matured cortical cells were defined as the cells within regions of fully developed root hairs (Pacheco-Escobedo et al., 2016). The RAM length was defined as the distance between quiescent center and first elongating cortical cells and the number of cortical cells within the RAM length were counted using the cell counter ImageJ plugin (https://imagej.nih.gov/ij/plugins/cell-counter.html) and regarded as the number of cells in the RAM (Pacheco-Escobedo et al., 2016).

### 2.8 Dry weight measurement

To obtain root and rosette leaf samples for dry weight measurement, surface sterilized seeds were first grown on rockwool with ultra-pure water and incubated for 7 days at 22°C under a 10-hour light/14-hour dark cycle (short day) and 70% relative humidity. Seedlings were transferred to liquid MGRL media containing 0.15 µM boric acid (low boron), 0.3 µM boric acid (mildly low boron) and 100 µM boric acid (normal boron) and grown for 28 days. Liquid culture was changed weekly during the initial 14 days after transfer, and subsequently changed twice in a week. The rosette leaves and roots of plant lines were harvested and rinsed with ultra-pure water. They were dried at 60°C for 15 days and the dry weight of both rosette leaves and roots was measured.

### 2.9 Cell wall extraction from root samples

For the analysis of cell wall properties, plants were grown in solid media containing 0.1 µM boric acid (low boron), 0.3 µM boric acid (mildly low boron) and 100 µM boric acid (normal boron) for 9 days and alcohol insoluble residues (AIR) were extracted from their frozen root as described (Matsunaga et al., 2004). About 600-900 root samples were harvested as a single sample for low boron condition and about 300-450, as a single sample for mildly low boron and normal boron conditions. The frozen root tissues were crushed at 1700 rpm for 15 sec in a total of 4 cycles using a multi bead shocker (YASUI KIKAI) and then homogenized with 80% (v/v) ethanol. The

homogenates were shaken using a rotator and centrifuged. The insoluble pellets were washed twice with 80% (v/v) ethanol, once with 99.5% (v/v) ethanol, twice with methanol/chloroform (1:1, v/v), once with acetone and twice with ultrapure water. The insoluble residues obtained were freeze-dried using FDU-1200 (EYELA, Japan) for 25 h and treated as cell wall samples.

### 2.10 Measurement of boron and calcium concentration

To measure total boron and calcium concentration in the rosette leaves and roots, plants were grown in a hydroponic culture system (the same system as dry weight measurement) under 0.1 µM boric acid (low boron), 0.3 µM boric acid (mildly low boron) and 100 µM boric acid (normal boron) and grown for 42 days (7 days in ultra-pure water and 35 days in liquid MGRL media). The concentration for low boron was increased to 0.15 µM boric acid after 19 days of culture in liquid MGRL media due to the severity of boron deficiency. The rosette leaves and roots were then harvested and rinsed with ultrapure water. The harvested samples were dried at 60 °C for 9 days (at least more than 3 days) and dry weight was measured. The dried samples were submerged in concentrated $HNO_3$ for 3 days at room temperature and first digested at 110 °C for about 2 h followed by digestion with $H_2O_2$ for 10 mins. The digested samples were dissolved in 2% $HNO_3$. For the measurement of cell wall boron and calcium concentration, about 2 mg of root AIR extracted from 9-d-old plants were treated with $HNO_3$ at room temperature for 3 days. The samples were then digested and dissolved in 2% $HNO_3$ as described above. Boron and calcium concentrations were measured by inductively coupled plasma mass spectrometry (ELAN DRC-e, PerkinElmer, USA).

### 2.11 Measurement of RG-II specific sugars

To estimate the amount of RG-II present in root cell wall of plant lines, the measurement of 2-keto-3-deoxy sugars as RG-II specific sugars was performed following a modified thiobarbituric

acid protocol described by York et al. (1985). About 1.5 mg of AIR were treated with 5 U of endo-polygalacturnanase from *Pectobacterium carotovorum*, (E-PGALPC, Megazyme, Ireland) in 300 µL of 0.1 M sodium acetate buffer at pH 5.5 for 89 h at 40 °C for complete digestion. The enzyme was dialyzed in 0.1 M sodium acetate buffer before use. The suspension was centrifuged three times to remove insoluble residues completely and the supernatant was collected after each centrifuge. To hydrolyze the polysaccharide sugar, 200 µL of the supernatant was mixed with 100 µL of 0.5 M $H_2SO_4$, vortexed and incubated at 100 °C for 30 mins. This was followed by cooling down the solution at room temperature for 10 mins, then the addition of 250 µL of 40 mM $HIO_4$ dissolved in 62.5 mM $H_2SO_4$, vortexing and incubation at room temperature for 20 mins for a cleavage reaction to generate formylpyruvic acid. 600 µL of 2% $Na_2SO_3$ dissolved in 0.5 M HCl was subsequently added to neutralize excess $HIO_4$ and vortexed. A brown coloration was formed upon this addition but quickly disappeared. 500 µL of 25 mM thiobarbituric acid was added, and the mixture was vortexed and incubated at 100 °C for 15 mins for pigment generation. 1 mL of DMSO (99.5%) was added to the solution for pigment stabilization and then the mixture was incubated at 24 °C for 7 mins. To quantify generated pigments, an absorbance at 548 nm was measured using a spectrophotometer (U-2910, HITACHI High Technologies Corp., Japan). The concentration of 2-keto-3-deoxy sugars were estimated using 2-keto-3-deoxyoctonate ammonium salt (Sigma-Aldrich, USA) as a standard.

### 2.12 Statistical analysis

Comparisons between the wildtype Col-0 and *avp2;1* mutants were performed using the Dunnett's test and Student's t-test.

# 3 Results

## 3.1 Mutations in *AVP2;1* increased primary root length under low boron

To explore the factors that modulate root growth under boron limitation, *A. thaliana* mutants were screened which showed increased primary root length under low boron supply from EMS-treated Col-0. One of these mutants named number 31A, represented as *avp2;1-4*, showed an enhanced primary root length under a limited supply of boron (0.06 µM and 0.1 µM, Figures 1A, D) although the primary root length was not statistically different from Col-0 under normal boron condition (100 µM, Figures 1A, D). Through genetic mapping and genomic sequencing, it was revealed that the longer primary root was caused by a single recessive locus and this mutant was found to carry a missense mutation in the 7$^{th}$ exon of *AVP2;1* which encodes a Golgi-localized proton pyrophosphatase (Figure 1B). This missense mutation (G800A in CDS) led to an amino acid substitution of glycine to aspartic acid (G267D in protein). G267 is predicted to be located close to the 6th transmembrane domain, and is conserved among AVP1, AVP2;1 and AVP2;2 (Segami et al., 2010; Tojo et al., 2023). To examine if the mutant phenotype was because of its mutation in *AVP2;1*, two T-DNA lines of *AVP2;1* were obtained. These two lines represented as *avp2;1-2* and *avp2;1-3* respectively, carry a T-DNA insertion in the 6$^{th}$ intron of *AVP2;1* (Figure 1B). Both T-DNA lines showed increased primary root under low boron but no differences under normal boron supply similar to *avp2;1-4* (Figures 1A, D), supporting that the mutations in *AVP2;1* were responsible for the increased primary root length under low boron conditions.

To check *AVP2;1* mRNA expression in the mutants, *AVP2;1* mRNA was quantified by qRT-PCR using two sets of primers to detect the upstream portion (5', exon 3-4) and downstream (3', exon 14-15) of T-DNA insertion. In Col-0, with the use of both sets of primers, *AVP2;1* mRNA level was not obviously changed under various boron concentrations (Figure 1C) suggesting that the mRNA expression of *AVP2;1* in roots is not dependent on boron nutrition.

Under low (0.1 µM) and normal (100 µM) boron, *AVP2;1* mRNA was not changed in *avp2;1-4* when compared to Col-0 using both upstream and downstream primers. However, in *avp2;1-2* and *avp2;1-3*, *AVP2;1* mRNA was reduced to 60% in the upstream portion of the T-DNA insertion. In the downstream portion of insertion, *AVP2;1* mRNA level was reduced to 0.5% and 7-10% in *avp2;1-2* and *avp2;1-3*, respectively under both boron conditions compared to Col-0 (Figure 1C). This suggests that although the destabilized 5' incomplete portion of mRNA was likely expressed, *AVP2;1* mRNA is not at least overexpressed in T-DNA insertion lines. This shows that the T-DNA insertion mutants, *avp2;1-2* and *avp2;1-3*, are knockdown mutants suggesting that reduced function of AVP2;1 is responsible for the mutant phenotype.

To examine the growth response of the *avp2;1* mutants to different boron conditions, plants were grown under various range of boron concentration. *avp2;1* mutants exhibited longer primary roots only under low boron conditions (0.06 and 0.1 µM) compared to Col-0 but showed no significant differences under mildly low (0.2 and 0.3 µM), normal (100 µM) and even toxic (3000 µM) boron conditions (Figure 1D).

Previous studies have shown that even at boron concentrations that do not affect vegetative growth, boron deficiency often affects the reproductive growth and fertility of the plant suggesting a higher boron requirement in the reproductive growth stage of plants (Dell and Huang, 1997). With the aim of checking the effect of *AVP2;1* mutation on plant fertility, the reproductive growth of wildtype and mutants under long day condition was examined. This was performed using a liquid culture method and like the solid media culture, *avp2;1* mutants showed longer root growth under low boron condition (0.1 µM), and no obvious differences under mildly low (0.3 and 0.5 µM), and normal boron (100 µM), conditions (Figure 2A). Inhibited internode elongation and fertility loss (assessed by presence/ number of siliques) were observed in both wildtype Col-0 and *avp2;1* mutants under low boron (0.1 µM) and mildly low boron (0.3 µM) conditions however, these symptoms were recovered in *avp2;1* mutants under 0.5 µM, a mildly low boron condition

although the number of stems seemed reduced in mutant lines (Figure 2B). Under normal boron condition, no major differences were observed in both vegetative and reproductive growth of wildtype Col-0 and *avp2;1* mutants (Figure 2). These results suggest that AVP2;1 likely affects the normal growth in both vegetative and reproductive stages of the plants under low boron conditions. This could be because of increased soluble boron (enough to meet the high demand of boron in the reproductive growth) due to a reduced boron binding capacity by *AVP2;1* mutation. Hence, the mutant lines can set seeds even under low boron condition (clearly seen under 0.5 µM). Also, AVP2s are generally abundant in flowers and siliques in addition to young roots.

To check the possibility of the involvement of *AVP2;1* in root growth under other stress conditions, mutant lines were grown under low phosphorus and low pH, respectively. No differences were found between the *avp2;1* mutants and Col-0 under these conditions (Figures 3A, B). Taken together, these results indicate that the reduced expression or function of *AVP2;1* causes an increase in the primary root length under a limited supply of boron and this increase is likely observed specifically under low boron.

### 3.2 Alleviated inhibition of both cell division and elongation was observed in *avp2;1* mutants

To characterize the effects of *avp2;1* mutations on root cells, the root tips of 5-d-old plants grown under low (0.1 µM), mildly low (0.3 µM), and normal (100 µM) boron were first observed under a stereomicroscope. Although primary root length was not obviously different between Col-0 and *avp2;1* mutants at this age under all the boron conditions (Figure 4A), longer meristematic and elongation zones were observed in *avp2;1* mutants compared to Col-0 under low (0.1 µM) boron condition (Figure 5A) and no difference was observed under mildly low (0.3 µM) boron (Figure 4B) and normal (100 µM) boron condition (Figure 5B). There were also no distinguishing differences in the root hair distribution between wildtype Col-0 and *avp2;1* mutant lines under

both low and normal boron conditions. The root cells of Col-0 and *avp2;1-4* mutant was further examined using a confocal microscope in 5-d-old plants. Under low (0.1 µM) boron, the shape of the root cells of Col-0 were collapsed and the root cell arrangement was damaged; however, *avp2;1-4* root cells showed a mitigated inhibition in cell shape and cell arrangement (Figure 5B). In addition, an increase in meristematic zone length, cell number in root apical meristem (RAM), and length of matured cortical cell was observed in *avp2;1-4* compared to Col-0 under low boron condition, and no differences was found under normal (100 µM) boron condition (Figure 5C). These observations suggest that inhibition of both root cell elongation and division caused by low boron was alleviated by *avp2;1* mutation accounting for the enhanced primary root growth.

### 3.3 Boron concentration in roots and rosette leaves was not different between Col-0 and *avp2;1* mutants

To explore the mechanisms behind the increased root length of *avp2;1* mutants under limited supply of boron, the possibility of an enhancement in boron uptake or transport in mutant lines was considered. To measure tissue boron concentration, plants were hydroponically grown so that plant roots can freely access the media. In hydroponic culture, *avp2;1* mutants also exhibited longer root length compared to the wildtype Col-0 under low (0.15 µM) boron condition when Col-0 root elongation was inhibited. No obvious difference in root length was found among plant lines under mildly low (0.3 µM) and normal (100 µM) boron conditions (Figure 6A). This shows the consistency of the mutant phenotype irrespective of the plant culture system. In both root and rosette leaf dry weight, no significant differences were observed between Col-0 and *avp2;1* mutants (Figure 6B). In the concentration of total boron in roots and rosette leaves, no differences were observed between the wildtype Col-0 and *avp2;1* mutant lines irrespective of the boron concentration in the media (Figure 6C). This suggests that the mutations in *AVP2;1* did not primarily affect the boron transport.

To further examine the effects of *avp2;1* mutation in boron transport, the mRNA expression of *NIP5;1*, *BOR1* and *BOR2* were checked in wildtype Col-0 and *avp2;1* mutant lines under low (0.1 µM) and normal (100 µM) boron conditions. *NIP5;1*, *BOR1* and *BOR2* encode major boron transporters required for root growth under low boron (Onuh and Miwa, 2021). No increase was detected in the mRNAs of these transporter genes in the mutant lines under low and normal boron conditions (Figures 7A-C). *NIP5;1* mRNA is induced by low boron (Tanaka et al., 2011). *NIP5;1* mRNA levels in all the three *avp2;1* mutants were rather reduced to 73-74% of that of Col-0 under low boron (Figure 7A). This decrease in *NIP5;1* mRNA in roots could be an indirect consequence of the increased root length in *avp2;1* mutants under low boron (Figure 1A). *NIP5;1* promoter activity is more strongly detected in the elongation zone compared to the mature portion of the roots (Takano et al., 2006). Compared to Col-0 in which root elongation was severely inhibited (Figure 1A), the relative proportion of the elongation zone to the entire root could be smaller in *avp2;1* mutants, resulting in the reduction in relative level of *NIP5;1* mRNA under low boron. Another possibility is as a result of the effect of cytosolic boric acid on *NIP5;1* mRNA because it has been known that cytosolic boric acid induces ribosome stalling and subsequent *NIP5;1* mRNA degradation (Tanaka et al., 2016). Later in this study, it is suggested that *AVP2;1* mutations likely reduce boron binding capacity in root cell wall due to decreased RG-II, which implies that cytosolic boric acid could be locally increased in mutant root cells, hence the decrease of *NIP5;1* mRNA.

Taken together, these results suggest that the upregulation of boron transport was not likely the cause of the enhanced root length exhibited by the *avp2;1* mutant lines under low boron.

### 3.4 Reduced calcium and RG-II specific sugars were observed in root cell wall of *avp2;1* mutants

Due to the role of boron in plant cell wall stability by crosslinking of two monomers of RG-II, changes in cell wall components were considered as a possible mechanism of the enhanced root growth of *avp2;1* mutants under a low boron supply. To explore this possibility, concentrations of the cell wall minerals, calcium, and boron, were measured in root cell wall under low (0.1 µM), mildly low (0.3 µM), and normal (100 µM) boron conditions. No difference was found in boron concentration in cell wall under low and mildly low boron condition, but *avp2;1* mutant lines showed a slight tendency of reduction compared to the wildtype Col-0 under normal boron conditions (Figure 8A). Since boron binding to RG-II is assumed to be saturated when sufficient boron is supplied, this suggests a possibility of a reduced boron binding capacity in *avp2;1* mutant cell wall. On the other hand, the concentration of calcium in the cell wall was generally increased in all the plant lines under low boron compared to mildly low and normal boron (Figure 8B), probably as a compensation of the reduced borate crosslinking in the cell wall. Under low boron, *avp2;1* mutant lines showed a significant decrease by 15-18% in cell wall calcium concentration (Figure 8B), but there were no differences under mildly low and normal boron conditions.

To further confirm the possibility of a reduced boron binding capacity in *avp2;1* mutant root cell wall, RG-II amount was estimated by measuring 2-keto-3-deoxy sugars which are RG-II specific sugars. There was a 6-17% decrease of RG-II specific sugars in *avp2;1* mutant lines compared to wildtype Col-0 under all the three boron conditions although a statistical difference was found only in *avp2;1-4* under low B (Figure 8C).

These results support that a*vp2;1* mutations did affect cell wall components and possibly cell wall stability. This change could probably explain the increased root growth of *avp2;1* mutants under a limited boron supply.

### 3.5 Mutations in *AVP2;2* and *AVP1* did not affect plant growth under low boron conditions

Recall that there are two types of proton translocating inorganic pyrophosphatase ($H^+$ -PPase); type I encoded by AVP1 and type II encoded by AVP2;1 and AVP2;2 in *A. thaliana*. AVP2;1 share 94% and 33% amino acid identity with AVP2;2 and AVP1 respectively. Due to the amino acid similarities between AVP2;2 and both AVP2;2 and AVP1 respectively, the likelihood that mutations in AVP2;2 and/or AVP1 may ameliorate low-boron stress was considered. To this end, growth analysis of *avp2;2* mutants and *avp1* mutants under different boron conditions was examined.

Homozygous T-DNA mutant lines of *AVP2;2* (*avp2;2-2* and *avp2;2-1*) together with *AVP2;1* T-DNA lines (*avp2;1-2* and *avp2;1-3*) and Col-0 seedlings were grown under low boron conditions (0.06 µM B and 0.1 µM B) and normal boron condition (100 µM B) for examination of their primary root length. Result revealed that there was no significant difference between the primary root length of *AVP2;2* T-DNA mutant lines and Col-0 under low boron condition (Figure 9A-B). Also, the primary root length of *AVP2;1* mutant lines were significantly longer than the primary root length of *AVP2;2* mutant lines under low boron conditions (Figure 9A-B). The analysis also showed that there was no significant differences in the primary root length of all seed lines under normal boron condition (Figure 9A-B).

A growth test was also performed using homozygous T-DNA mutant lines of *AVP1* (*avp1-4*) together with *AVP2;1* T-DNA lines (*avp2;1-2* and *avp2;1-3*) and Col-0 seedlings. Mutants and wildtype plants were grown under low boron conditions (0.06 µM B and 0.1 µM B) and normal boron condition (100 µM B) for examination of their primary root length. Similar to the growth test with *avp2;2* mutants, the result revealed that while *avp2;1* mutants (*avp2;1-2* and *avp2;1-3*) longer primary root length under low boron conditions compared to wildtype Col-0, *avp1* mutant

(*avp1-4*) did not (Figure 10A-B). Also, there were no significant differences in the primary root length of all seed lines under normal boron condition (Figure 10A-B). These results suggest that increases in primary root length under low boron conditions are specifically observed in *avp2;1* mutants. AVP1 and AVP2;2 may probably not be involved in root growth under low boron condition due to differences in subcellular localization (AVP1) and protein abundance (AVP2;2). Subcellular localization does impact protein function and although AVP1 and AVP2;1 share the same biochemical function as $H^+$-PPases, a mutation in AVP1 (localized to the vacuole) may not cause a distinguishing phenotype under low boron condition like AVP2;1 (localized to the Golgi apparatus). This is because the function site of boron is in pectin, which is synthesized in the Golgi apparatus hence, the possible role of AVP2;1 (localized to the Golgi apparatus) in low boron stress. Compared to AVP2;1, AVP2;2 has a very negligible protein abundance and although both are localized to the Golgi apparatus, the negligible protein abundance of AVP2;2 could have no distinguishing effects on root growth under low boron condition.

## 4 Discussion

Previous studies have successfully identified and characterized the *A. thaliana* type II $H^+$-PPase, AVP2;1 as a proton pump localized to the Golgi apparatus and TGN (Segami et al., 2010). However, its physiological role and their mutant phenotype remains poorly understood in plants. In this study, *avp2;1* mutants were characterized from the view of boron deficiency stress, and it was found that mutations in *AVP2;1* affected plant growth under low boron conditions and cell wall components under low and normal boron conditions. Indeed, the point mutation mutant *avp2;1-4* showed a more significant response to low boron in root growth (Figure 1) and RG-II reduction (Figure 8) compared to T-DNA lines *avp2;1-2* and *avp2;1-3*. One possible explanation for this could be the effect of other mutations present in *avp2;1-4*. This is assumed because the mutagen used in generation of *avp2;1-4* is EMS which introduces multiple point mutations in a mutant. Another possibility is the possible remain of some amount of AVP2;1 protein in the T-DNA lines. This is assumed based on the detection of some amount of *AVP2;1* mRNA in the 5' proportion of *AVP2;1* in T-DNA mutants confirming that T-DNA lines are knock down mutants. Finally, it is also possible that the introduction of T-DNA into *AVP2;1* may have also affected some portion of the neighboring genes hence their weaker phenotype compared to *avp2;1-4*. However, based on the similar phenotype exhibited by the mutants under low boron condition, it can be concluded that the phenotypes were as a result of *AVP2;1* mutation. To describe the mechanism behind the observed phenotypes, it is proposed that a reduction of AVP2;1 decreases pH pumping activity in Golgi apparatus, and this possibly leads to the changes in biological processes in Golgi apparatus such as reduction in pectin synthesis, which causes reduced sensitivity to low boron by a reduced boron requirement.

### 4.1 $H^+$ pumping rather than PPi hydrolysis is likely the connector of AVP2;1 to enhanced root growth under low boron condition

AVP2;1 like other $H^+$ -PPases has the dual role of PPi hydrolysis and proton pumping. To have a holistic picture of the functioning of AVP2;1 in plants, it is important to understand which role of AVP2;1 leads to the observed mutant phenotypes. In the case of AVP1/VHP1, *fugu5* mutant was used to demonstrate this. The *fugu5-1* is a loss-of-function *AVP1* mutant which has a null PPase activity resulting in reduced shoot growth, impaired size and shape of cotyledon, and reduced hypocotyl length of etiolated seedlings (Ferjani et al., 2011; Asaoka et al., 2016). The introduction of cytosolic soluble inorganic pyrophosphatase (IPP) of *S. cerevisiae* under the control of the *AVP1* promoter into the *fugu5-1* mutant, was able to rescue these phenotypes (Ferjani et al., 2011). This suggested that rather than proton pumping, hydrolysis of cytosolic PPi is the major physiological role of AVP1. This was further confirmed using an uncoupling mutated variant of AVP1 that could hydrolyze PPi but had no proton pumping activity. The introduction of this mutant variant into *fugu5-3* rescued shoot growth as when native $H^+$-PPase (AVP1) was introduced (Asaoka et al., 2016), thereby supporting that the hydrolytic role rather than proton pumping of AVP1, is essential for plant growth. On the other hand, Tojo et al (2023) has revealed the negligible contribution of PPi hydrolytic role of AVP2;1 in growth of *A. thaliana* seedling. This was done by phenotypic characterization of the *AVP2;1* mutant, *vhp2;1-1*/*avp2;1-1* (SAIL_512_B02) and *fugu5-1vhp2;1-1* double mutant. Phenotypes related to loss of PPase activity such as alterations in cotyledon shape and hypocotyl elongation defects in etiolated seedlings were not observed in *vhp2;1-1* and neither was any additional effect observed in *fugu5-1vhp2;1* compared to *fugu5-1*. When the response of *avp1-4* (Yang et al., 2018) to low boron stress was tested, no difference from Col-0 was observed in contrast to *avp2;1* mutants (Figure 10). Considering the minimal contribution of AVP2;1 in PPi hydrolysis for the growth of *A.*

*thaliana* and the plant growth observed in *avp1-4*, it is suggested that rather than the hydrolysis of cytosolic PPi, proton pumping into the Golgi apparatus may be the connector of AVP2;1 to enhanced root growth under low boron condition.

### 4.2 Change of $H^+$ pumping activity in the Golgi apparatus possibly affects pectin synthesis

The Golgi apparatus is involved in sorting and transporting proteins to cellular compartments as well as assembling and exporting the non-cellulosic polysaccharides of the cell wall matrix including pectin in plants (Driouich et al., 2012). For non-cellulosic cell wall polysaccharide synthesis in Golgi apparatus, by the activity of the nucleotide sugar transporter (NST), nucleoside di-phosphate sugar (NDP-sugar) is imported from the cytosol into the Golgi lumen, supplying substrate for glycosyltransferase (Figure 11). The sugar moiety is then transferred to a building chain of polysaccharide via the action of glycosyltransferase and the resulting NDP is hydrolyzed by NDPase to nucleoside monophosphate (NMP) and inorganic phosphate. The NMP concentration gradient drives transport of NDP-sugar via NSTs as NDP-sugar/NMP antiporters. The inorganic phosphate released from NDP hydrolysis is exported into the cytosol from Golgi apparatus via a phosphate transporter (Reyes and Orellana 2008; Figure 11).

Assuming $H^+$ pumping activity of AVP2;1 as the connection to the enhanced root growth of mutants under low boron condition, it is proposed that a reduced function of AVP2;1 would increase pH and affect ion homeostasis in the Golgi apparatus. The effect of these changes would likely affect biochemical processes in the Golgi apparatus including pectin synthesis (Figure 11) and in this study, a tendency of a reduction in RG-II amount has been observed under various boron concentrations in *avp2;1* mutant cell wall (Figure 8). This proposition is in line with Reyes and Orellana (2008) hypothesis that the activity of glycosyltransferase could be affected by ion homeostasis and pH. pH dependent activity of some *A. thaliana* glycosyltransferases such as RG-I: galacturonsyltransferase (RGGAT1) (Amos et al., 2022), HG: galacturonosyltransferase

(GAUT1:GAUT7) (Amos et al., 2018), RG-I: rhamnosyltransferase (RRT1) (Takenaka et al., 2018), RG-II: xylosyltransferase (RGXT1) (Petersen et al., 2009) involved in pectin synthesis has been reported. These in vitro analyses showed an optimal pH for these glycosyltransferases to be pH 6.5 (RGGAT1), pH 7.2 (GAUT1:GAUT7), pH 7 (RRT1) and around pH 7 (RGXT1). However, this may be different from the actual activity within the cell considering the pH range of the Golgi apparatus. In addition, it has been shown in human cancer cells that a slight increase in the Golgi pH affects the formation of glycosyltransferase complexes and induces mislocalization of glycosyltransferase from the Golgi apparatus into endosomal compartments (Kellokumpu, 2019).

The Golgi-localized inorganic phosphate transporter, PHT4;6 in *A. thaliana* has been identified to release inorganic phosphate (Pi) into the cytosol from the Golgi lumen (Guo et al., 2007). Although it has not been experimentally demonstrated, it is hypothesized that the release of the lumenal Pi by PHT4;6 is dependent on proton gradients (Guo et al., 2007). The lumenal Pi if not released, could hamper activities in the Golgi apparatus including pectin synthesis.

Considering the localization of AVP2;1 to the TGN, there is also a possibility that the pectin trafficking is hampered/affected by a reduced function of AVP2;1. This probably could lead to a reduced amount of pectin which is trafficked or deposited to the cell wall.

The reduction of calcium concentration was also observed in cell wall of *avp2;1* mutants under low boron compared to wildtype Col-0 (Figure 8). The HG is crosslinked by calcium and hence, a reduction in cell wall calcium concentration could imply a reduced HG. It is proposed that in addition to RG-II polysaccharide, HG polysaccharide could be also affected by changes in the state of the Golgi apparatus caused by the reduced $H^+$ pumping activity of AVP2;1. It is also possible that the reduction of calcium-crosslinked HG is due to a secondary effect induced by growth change in mutants rather than a direct effect of reduction in $H^+$ pumping activity of AVP2;1. Pectin methylesterase (PME) catalyzes the demethylesterification of HG thereby

increasing calcium crosslinking. It has been found that the activity of PME is induced by boron deficiency (Yan et al., 2021) possibly for compensation of borate-RG-II crosslinking. Hence, due to relieved severity of boron deficiency in *avp2;1* mutants under low boron supply, the demethylesterification activity of the PME could be reduced resulting in the decrease of cell wall calcium concentration.

### 4.3 Decrease in RG-II amount may possibly reduce boron requirement in *avp2;1* mutants

One of the major effects of boron deficiency on plants is the damage of growing points, which include inhibition of root cell elongation and division leading to a cessation of root elongation (Dell and Huang, 1997). However, *avp2;1* mutant lines showed less sensitivity to this (Figures 1, 2 and 5). Following the observed tendency of reduced amount of RG-II by 6-17 % in these mutants (Figure 8), it is suggested that this reduced sensitivity to low boron is because of a reduction in boron requirement. Reduced boron requirement means that a smaller amount of boron can satisfy the boron demand possibly due to the reduced boron binding sites for RG-II in *avp2;1* mutants. In line with our study, Hiroguchi et al. (2021) has also shown that 20-30% reduction in RG-II enhances root elongation under limited supply of boron. In this case, increased root meristem was not clearly observed under low boron condition in *tmn1* mutants at 4 days compared to this current study of *avp2;1* mutants at 5 days (Figure 5). However, a tendency of an increased root meristem was observed in the *tmn1* mutant still at 4 days and at a longer incubation time under low boron condition in hydroponic culture (Hiroguchi et al., 2021).

It has also been reported that there is a positive correlation between pectin amount and cell wall boron concentration which may represent amount of boron required by plants for tissue development among different plant species (Hu et al., 1996). More directly, a positive correlation between cell wall boron concentration and RG-II amount has been revealed (Matoh et al., 1996). This implies pectin amount or RG-II amount determines sensitivity to boron deficiency hence the

reduced sensitivity to low boron in *avp2;1* mutants. It is suggested that cell wall modification would be another approach for conferring low-boron tolerance.

### 4.4 The contribution of AVP2;1 to pH homeostasis in Golgi apparatus may be minimal

In our study, *avp2;1* mutants showed a significant increase in primary root growth accompanied by increased root cell division and elongation when compared to wildtype Col-0 under low boron. This increment of growth was however not observed in the leaves of *avp2;1* mutants (Figures 1, 6) possibly because AVP2s protein is predominately expressed in roots but not in young and mature leaves (Segami et al., 2010). Again, differences between the wildtype Col-0 and *avp2;1* mutants were not observed under normal boron condition. One possible explanation to this could be a minor contribution of AVP2;1 to pH homeostasis in Golgi apparatus because it is assumed that V-ATPase is the major proton pump in the Golgi apparatus. Result of the analysis of RG-II specific sugars revealed a 6-7% consistent reduction in *avp2;1* mutants compared to wildtype Col-0 under both low and normal boron condition except for *avp2;1-4* which showed 17% reduction under low boron condition. Under normal boron conditions, most of RG-II is crosslinked by sufficient supply of boron therefore, a 6-7% reduction of RG-II may not greatly affect the plant growth. However, under low boron conditions, when borate crosslinking of RG-II is likely a major determinant for cell division and elongation, this slight change of RG-II could affect the plant growth.

AVP2;2 is an isoform of AVP2;1 and shares about 94% amino acid sequence identity (Segami et al., 2010). Based on the amino acid sequence identity of the two proteins, *avp2;2* mutants were examined to check if AVP2;2 has a similar role in low boron as AVP2;1. The analysis of the growth of *avp2;2* mutants, however, revealed that unlike *avp2;1* mutants, *avp2;2* mutants showed no significant differences from Col-0 under low and normal boron conditions (Figure 9). This could be because of its very low transcript amount compared to *AVP2;1* hence

no noticeable change in *avp2;2* mutants. Another possibility is that though AVP2;1 and AVP2;2 share great similarities, their functions do not overlap, and reduction of low boron sensitivity may be specific to AVP2;1.

In conclusion, this study supports an idea that AVP2;1 plays a role in proton pumping and acidification of Golgi apparatus for maintenance of pectin synthesis by examination of *avp2;1* mutants. It also proposes the reduction of boron requirement by molecular approach as a sustainable strategy against low boron stress. As a future perspective, analysis of other cell wall components such as HG and measurement of cell stiffness in plant lines will be helpful in providing further information on the effect of *AVP2;1* mutation on plants. Although a large difference (over 15%) between the Golgi pH in *avp2;1* mutants and wildtype is not expected, monitoring the Golgi pH in the plant lines will also increase and better validate the function of AVP2;1 in the maintenance of Golgi pH.

## 5 Acknowledgment

The accomplishment of this work was not only made possible by me, but also with the help of some people. First, I especially appreciate my supervisor Dr. Kyoko. Miwa, who helped guide me through this research and in whose laboratory and constant supervision, this work became a success. Her profound advice, constant support and warm encouragement were of great help and without her guidance, I would not have accomplished my study.

I am also grateful to Prof. Masaaki Morikawa, Prof. Ryouichi Tanaka and Associate Prof. Chiaki Hori for their very valuable suggestions and discussions as my referees in my Ph.D. defense.

I would also like to use this medium to express my gratitude to DX fellowship body and the body of Hokkaido University Special Grant Program for Self-supported International Students for their financial support. The financial support I obtained from these bodies was of great help and helped sustain me all through my Ph.D. research period.

I also sincerely appreciate Michiko Tsukamoto and Yuko Kawara for their technical assistance and Prof. Toshirio Watanabe for his technical support in ICP-MS.

My sincere gratitude also goes out to my past and present laboratory members for their constant support and help in areas where I needed assistance. They helped make my study in Japan, more comfortable and exciting.

This acknowledgment will not be complete without mentioning my friends and family. I want to appreciate first, my husband who has effectively stood by me through the tough and challenging times. My heartfelt gratitude to my family in Nigeria and my friends (here in Japan and Nigeria) for their immense support, prayers, and provision during the course of this study. They were a strong emotional pillar for me. Words are not enough to say how grateful I am.

Finally, and most importantly, everything I have achieved is by the grace of God Almighty and I would like to express my gratitude to Him, for His grace and mercy that sustained and carried me throughout my Ph.D. journey.

## 6 References


Alba, K., and Kontogiorgos, V. (2017). Pectin at the oil-water interface: Relationship of molecular composition and structure to functionality. *Food Hydrocoll. 68*, 211–218. doi.10.1016/j.foodhyd.2016.07.026

Alonso, J. M., Stepanova, A. N., Leisse, T. J., Kim, C. J., Chen, H., Shinn, P., et al. (2003). Genome-wide insertional mutagenesis of *Arabidopsis thaliana*. *Science* 301, 653–657. doi.10.1126/science.1086391

Amos, R. A., Atmodjo, M. A., Huang, C., Gao, Z., Venkat, A., Taujale, R., et al. (2023). Polymerization of the backbone of the pectic polysaccharide rhamnogalacturonan I. *Nat. Plants* 4, 673. doi.10.1038/s41477-022-01270-3

Amos, R. A., Pattathil, S., Yang, J. Y., Atmodjo, M. A., Urbanowicz, B. R., Moremen, K. W., et al. (2018). A two-phase model for the non-processive biosynthesis of homogalacturonan polysaccharides by the GAUT1:GAUT7 complex. *J. Biol. Chem*. 49, 19047–19063. doi. 10.1074/jbc.RA118.004463

Asaoka, M., Segami, S., Ferjani, A., Maeshima, M. (2016). Contribution of PPi-hydrolyzing function of vacuolar $H^+$-pyrophosphatase in vegetative growth of *Arabidopsis*: Evidenced by expression of uncoupling mutated enzymes. *Front. Plant Sci.* 7, 415. doi.10.3389/fpls.2016.00415

Cosgrove, D. J., and Jarvis, M. C. (2012). Comparative structure and biomechanics of plant primary and secondary cell walls. *Front. Plant Sci.* 3, 204. doi.10.3389/fpls.2012.00204

Dannel, F., Pfeffer, H., Römheld, V. (2002). Update on boron in higher plants - Uptake, primary translocation and compartmentation. *Plant Biol* 4, 193–204. doi.10.1055/s-2002-25730

Dell, B., and Huang, L. (1997). Physiological response of plants to low boron. *Plant Soil* 193, 103-120. doi.10.1023/A:1004264009230.

Driouich, A., Faye, L., Staehelin, A. (1993). The plant Golgi apparatus: a factory for complex polysaccharides and glycoproteins. *Trends Biochem. Sci.* 18, 210–214. doi.10.1016/0968-0004(93)90191-O

Driouich, A., Follet-Gueye, M. L., Bernard, S., Kousar, S., Chevalier, L., Vicré-Gibouin, M., et al. (2012). Golgi-mediated synthesis and secretion of matrix polysaccharides of the primary cell wall of higher plants. *Front. Plant Sci.* 3, 79. doi.10.3389/fpls.2012.00079

Drozdowicz, Y. M., Kissinger, J. C., Rea, P. A. (2000). AVP2, a sequence-divergent, $K^+$-insensitive $H^+$-translocating inorganic pyrophosphatase from Arabidopsis. *Plant Physiol*. 123, 353-362. doi.10.1104/pp.123.1.353

Duran, C., Arce-Johnson, P., Aquea, F. (2018). Methylboronic acid fertilization alleviates boron deficiency symptoms in *Arabidopsis thaliana*. *Planta* 248, 221–229. doi.10.1007/S00425-018-2903-0

Ferjani, A., Segami, S., Horiguchi, G., Muto, Y., Maeshima, M., Tsukaya, H. (2011). Keep an eye on PPi: The vacuolar-type $H^+$-pyrophosphatase regulates postgerminative development in *Arabidopsis*. *Plant Cell* 23, 2895–2908. doi.10.1105/tpc.111.085415

Fujiwara, T., Hirai, M. Y., Chino, M., Komeda, Y., Naito, S. (1992). Effects of sulfur nutrition on expression of the soybean seed storage protein genes in transgenic petunia. *Plant Physiol.* 99, 263-268. doi.10.1104/pp.99.1.263

Fujiyama, B. S., Silva, A. R. B., Silva Júnior, M. L., Cardoso, N. R. P., Fonseca, A. B., Viana, R. G., et al. (2019). Boron fertilization enhances photosynthesis and water use efficiency in soybean at vegetative growth stage. *J. Plant Nutr.* 42, 2498–2506. doi.10.1080/01904167.2019.1659326

Güneş, A., Alpaslan, M., İnal, A., Sait Adak, M., Eraslan, F., Çiçek, N. (2003). Effects of boron fertilization on the yield and some yield components of bread and durum wheat. *Turk. J. Agric.* 27, 329-335.

Guo, B., Jin, Y., Wussler, C., Blancaflor, E. B., Motes, C. M., Versaw, W. K., Versaw, W. K. (2007). Functional analysis of the *Arabidopsis* PHT4 family of intracellular phosphate transporters. *New Phytol.* 177, 889–898. doi.10.1111/j.1469-8137.2007.02331.x

Gupta, U. C., Jame, Y. W., Campbell, C. A., Leyshon, A. J., Nicholaichuk, W. (1985). Boron toxicity and deficiency: a review. *Can. J. soil sci.* 65, 381-409. doi.10.4141/cjss85-044

Hiroguchi, A., Sakamoto, S., Mitsuda, N., Miwa, K. (2021). Golgi-localized membrane protein AtTMN1/EMP12 functions in the deposition of rhamnogalacturonan II and I for cell growth in Arabidopsis. *J. Exp. Bot.* 72, 3611–3629. doi.10.1093/jxb/erab065

Hu, H., Brown, P. H., Labavitch, J. M. (1996). Species variability in boron requirement is correlated with cell wall pectin. *J. Exp. Bot.* 47, 227-232. doi.10.1093/jxb/47.2.227

Kellokumpu, S. (2019). Golgi pH, ion and redox homeostasis: how much do they really matter? *Front. Cell Dev. Biol.* 7, 93. doi.10.3389/fcell.2019.00093

Kim, Y. S., Kim, I. S., Choe, Y. H., Bae, M. J., Shin, S. Y., Park, S. K., et al. (2014). Overexpression of the *Arabidopsis* vacuolar $H^+$-pyrophosphatase AVP1 gene in rice plants improves grain yield under paddy field conditions. *J. Agric. Sci.* 152, 941–953. doi.10.1017/S0021859613000671

Kobayashi, M., Matoh, T., Azuma, J. I. (1996). Two chains of rhamnogalacturonan II are cross-linked by borate-diol ester bonds in higher plant cell walls. *Plant Physiol.* 110, 1017–1020. doi.10.1104/pp.110.3.1017

Lerouxel, O., Cavalier, D. M., Liepman, A. H., Keegstra, K. (2006). Biosynthesis of plant cell wall polysaccharides - a complex process. *Curr. Opin. Plant Biol.* 9, 621–630. doi.10.1016/j.pbi.2006.09.009

Li, J., Yang, H., Peer, W. A., Richter, G., Blakeslee, J., Bandyopadhyay, A., et al. (2005). *Arabidopsis* $H^+$-PPase AVP1 regulates auxin-mediated organ development. *Science* 310, 121–125. doi.10.1126/science.1115711

Luo, Y., Scholl, S., Doering, A., Zhang, Y., Irani, N. G., Di Rubbo, S., et al. (2015). V-ATPase activity in the TGN/EE is required for exocytosis and recycling in *Arabidopsis*. *Nat. Plants* 1, 15094. doi.10.1038/nplants.2015.94

Matoh, T., Ishigaki, K., Ohno, K., Azuma, J. (1993). Isolation and characterization of a boron-polysaccharide complex from radish roots. *Plant Cell Physiol.* 34, 639–642. doi.10.1093/oxfordjournals.pcp.a078465

Matoh, T., Kawaguchi, S., Kobayashi, M. (1996). Ubiquity of a borate-rhamnogalacturonan II complex in the cell walls of higher plants. *Plant Cell Physiol.* 37, 636–640. doi.10.1093/oxfordjournals.pcp.a028992

Matsunaga, T., Ishii, T., Matsumoto, S., Higuchi, M., Darvill, A., Albersheim, P., et al. (2004). Occurrence of the primary cell wall polysaccharide rhamnogalacturonan II in pteridophytes, lycophytes, and bryophytes. implications for the evolution of vascular plants. *Plant Physiol.* 134, 339–351. doi.10.1104/pp.103.030072

Miwa, K., and Fujiwara, T. (2010). Boron transport in plants: Co-ordinated regulation of transporters. *Ann. Bot.* 105,1103–1108). doi.10.1093/aob/mcq044

Mohnen, D. (2008). Pectin structure and biosynthesis. *Curr. Opin. Plant Biol.* 11, 266–277. doi.10.1016/j.pbi.2008.03.006

Ndeh, D., Rogowski, A., Cartmell, A., Luis, A.S., Basle, A., Gray, J., et al. (2017). Complex pectin metabolism by gut bacteria reveals novel catalytic functions. *Nature* 544, 65–70. doi.10.1038/nature21725

Nepal, N., Yactayo-Chang, J. P., Gable, R., Wilkie, A., Martin, J., Aniemena, C. L., et al. (2020). Phenotypic characterization of *Arabidopsis thaliana* lines overexpressing AVP1 and MIOX4 in response to abiotic stresses. *Appl. Plant Sci.* 8, e11384. doi.10.1002/aps3.11384

O'Neill, M. A., Eberhard, S., Albersheim, P., Darvill, A. G. (2001). Requirement of borate cross-linking of cell wall rhamnogalacturonan II for *Arabidopsis* Growth. *Science* 294, 846–849. doi.10.1126/science.1062319

Onuh, A. F., and Miwa, K. (2021). Regulation, diversity and evolution of boron transporters in plants. *Plant Cell Physiol.* 62, 590–599. doi.10.1093/pcp/pcab025

Pacheco-Escobedo, M. A., Ivanov, V. B., Ransom-Rodríguez, I., Arriaga-Mejía, G., Ávila, H., Baklanov, I. A., et al. (2016). Longitudinal zonation pattern in *Arabidopsis* root tip defined by a multiple structural change algorithm. *Ann. Bot.* 118, 763–776. doi.10.1093/aob/mcw101

Petersen, B. L., Egelund, J., Damager, I. Kirsten, F., Jacob, K. J., Zhang, Y., et al. (2009). Assay and heterologous expression in *Pichia pastoris* of plant cell wall type-II membrane anchored glycosyltransferases. *Glycoconj. J.* 26, 1235–1246. doi.10.1007/s10719-009-9242-0

Raven, J. A. (1980). Short- and long-distance transport of boric acid in plants. *New Phytol*, 84, 231–249. doi.10.1111/j.1469-8137.1980.tb04424.x

Reyes, F., and Orellana, A. (2008). Golgi transporters: opening the gate to cell wall polysaccharide biosynthesis. *Curr. Opin. Plant Biol.* 11, 244–251. doi.10.1016/j.pbi.2008.03.008

Segami, S., Makino, S., Miyake, A., Asaoka, M., Maeshima, M. (2014). Dynamics of vacuoles and $H^+$-pyrophosphatase visualized by monomeric green fluorescent protein in *Arabidopsis*: Artifactual bulbs and native intravacuolar spherical structures. *Plant Cell* 26, 3416–3434. doi.10.1105/tpc.114.127571

Segami, S., Nakanishi, Y., Sato, M. H., Maeshima, M. (2010). Quantification, organ-specific accumulation and intracellular localization of type II $H^+$-pyrophosphatase in *Arabidopsis thaliana.* *Plant Cell Physiol.* 51, 1350–1360. doi.10.1093/pcp/pcq096

Sessions, A., Burke, E., Presting, G., Aux, G., McElver, J., Patton, D., et al. (2002). A high-throughput *Arabidopsis* reverse genetics system. *Plant Cell* 14, 2985–2994. doi.10.1105/TPC.004630

Shen, J., Zeng, Y., Zhuang, X., Sun, L., Yao, X., Pimpl, P., et al. (2013). Organelle pH in the *Arabidopsis* endomembrane system. *Mol. Plant* 6, 1419–1437. doi.10.1093/mp/sst079

Shorrocks, V. M. (1997). The occurrence and correction of boron deficiency. *Plant Soil*, 193, 121–148. doi.10.1007/978-94-011-5580-9_9

Takano, J., Wada, M., Ludewig, U., Schaaf, G., von Wirén, N., Fujiwara, T. (2006). The *Arabidopsis* major intrinsic protein NIP5;1 is essential for efficient boron uptake and plant development under boron limitation. *Plant Cell* 18, 1498–509. doi.10.1105/tpc.106.041640

Takano, J., Miwa, K., Fujiwara, T. (2008). Boron transport mechanisms: collaboration of channels and transporters. *Trends Plant Sci* 13, 451–457. doi.10.1016/j.tplants.2008.05.007

Takenaka, Y., Kato, K., Ogawa-Ohnishi, M., Tsuruhama, K., Kajiura, H., Yagyu, K., et al. (2018). Pectin RG-I rhamnosyltransferases represent a novel plant-specific glycosyltransferase family. *Nat. Plants* 4, 669–676. doi.10.1038/s41477-018-0217-7

Tanaka, M., Takano, J., Chiba, Y., Lombardo, F., Ogasawara, Y., Onouchi, H., et al. (2011). Boron-dependent degradation of *NIP5;1* mRNA for acclimation to excess boron conditions in *Arabidopsis*. *Plant Cell* 23, 3547–3559. doi.10.1105/tpc.111.088351

Tanaka, M., Sotta, N., Yamazumi, Y., Yamashita, Y., Miwa, K., Murota, K., et al. (2016). The minimum open reading frame, AUG-Stop, induces boron-dependent ribosome stalling and mRNA degradation. *Plant Cell* 11, 2830-2849. doi.10.1105/tpc.16.00481

Tojo, H., Tabeta, H., Gunji, S., Hirai, M. Y., David, P., Javot, H., et al. (2023). Roles of type II $H^+$-PPases and PPsPase1/PECP2 in early developmental stages and PPi homeostasis of *Arabidopsis thaliana*. *Front. Plant Sci.* 14, 1031426. doi.10.3389/fpls.2023.1031426

Voxeur, A., Soubigou-Taconnat, L., Legée, F., Sakai, K., Antelme, S., Durand-Tardif, M., et al. (2017). Altered lignification in *mur1-1* a mutant deficient in GDP-L-fucose synthesis with reduced RG-II cross linking. *PLoS ONE* 12, e0184820. doi.10.1371/journal.pone.0184820

Yan, L., Riaz, M., Liu, J., Liu, Y., Zeng, Y., Jiang, C. (2021). Boron reduces aluminum deposition in alkali-soluble pectin and cytoplasm to release aluminum toxicity. *J. Hazard. Mater.* 401, 123388. doi.10.1016/j.jhazmat.2020.123388

Yan, X., Wu, P., Ling, H., Xu, G., Xu, F., Zhang, Q. (2006). Plant nutriomics in China: An overview. *Ann. Bot., 98*, 473–482. doi.10.1093/aob/mcl116

Yang, Y., Tang, R.J., Mu, B., Ferjani, A., Shi, J., Zhang, H., et al. (2018). Vacuolar proton pyrophosphatase is required for high magnesium tolerance in *Arabidopsis*. *Int. J. Mol. Sci.* 19, 3617. doi.10.3390/ijms19113617.

York, W., Darvill, A. G., Mcneil, M., Albersheim., P. (1985). 3-deoxy-D-*manno*-2-octulosonic acid (KDO) is a component of rhamnogalacturonan II, a pectic polysaccharide in the primary cell walls of plants. *Carbohydr. Res.* 138, 109-126. doi.10.1016/0008-6215(85)85228-9

Zhang, H., Chen, M., Xu, C., Liu, R., Tang, W., Chen, K., et al. (2023). $H^+$-pyrophosphatases enhance low nitrogen stress tolerance in transgenic *Arabidopsis* and wheat by interacting with a receptor-like protein kinase. *Front. Plant Sci.* 14, 1096091. doi.10.3389/fpls.2023.1096091

Zhang, Y., Feng, X., Wang, L., Su, Y., Chu, Z., Sun, Y. (2020). The structure, functional evolution, and evolutionary trajectories of the $H^+$-PPase gene family in plants. *BMC Genom.*, 21, 195. doi.10.1186/s12864-020-6604-2

## 7 List of publications

Onuh, A. F., and Miwa, K. (2021). Regulation, diversity and evolution of boron transporters in plants. *Plant Cell Physiol.* 62, 590–599. doi.10.1093/pcp/pcab025

Onuh, A. F., and Miwa, K. (2023). Mutations in type II Golgi-localized proton pyrophosphatase *AVP2;1/VHP2;1* affect pectic polysaccharide rhamnogalacturonan-II and alter root growth under low boron condition in *Arabidopsis thaliana*. *Front. Plant Sci*. 14.1255486. doi.10.3389/fpls.2023.1255486

**Table 1. Primers used in this study**

| Stock no | **Sequence (5'>3')** | **Purpose** | **Product size** |
|---|---|---|---|
| **5** | ATTTTGCCGATTTCGGAAC | Genotyping of *avp2;1-2* SALK_0542912 (T-DNA LB) | ~500 bp |
| **654** | ATGCCCCAAACAAGGATGTCA | | |
| **653** | GGCTGTGATTGGTATCGCCA | Genotyping of *avp2;1-2* | 658 bp |
| **654** | ATGCCCCAAACAAGGATGTCA | SALK_0542912 (AT genome) | |
| **6** | TTCATAACCAATCTCGATACAC | Genotyping of *avp2;1-3* | ~513 bp |
| **654** | ATGCCCCAAACAAGGATGTCA | SAIL_165F07 (T-DNA LB) | |
| **653** | GGCTGTGATTGGTATCGCCA | Genotyping of *avp2;1-3* | 658 bp |
| **654** | ATGCCCCAAACAAGGATGTCA | SAIL_165F07 (AT genome) | |
| **1201** | CATCATCGTGTTCGTCTTCAC | *AVP2;1* mRNA quantification at 5' portion | 200 bp |
| **1202** | GAATCACAAAAGCTAGCAAAATG | | |
| **1203** | ATACATAGAGACCGGGGCACTT | *AVP2;1* mRNA quantification at 3' portion | 199 bp |
| **844** | AAGCCGGGATGGATAAGTAACG | | |
| **226** | AATCTCGCAGCGGAAACG | *BOR1* mRNA quantification | 141 bp |
| **227** | TGGAGTCGAACTTGAACTTGTC | | |
| **1199** | CATCTCGCAGTACCGGAAGCT | *BOR2* mRNA quantification | 218 bp |
| **1200** | AGCCTTGGACTCATCTCACCT | | |

| | | | |
|---|---|---|---|
| **139** | CACCGATTTTCCCTCTCCTGAT | *NIP5;1* mRNA quantification | 151 bp |
| **140** | GCATGCAGCGTTACCGATTA | | |
| **61** | CCTTGGTGTCAAGCAGATGA | *EF 1α* mRNA quantification | 102 bp |
| **62** | GAAGACACCTCCTTGATGATTT | | |
| **1049** | ATTGCTTTCGTGCTTGGTGC | Genotyping of *avp1-4* | 626 bp |
| **259** | ATATTGACCATCATACTCATTGC | GABI_596C07 (T-DNA LB) | |
| **1049** | ATTGCTTTCGTGCTTGGTGC | Genotyping of *avp1-4* | 641 bp |
| **1050** | AATGGGTAGCACATGGCAGT | GABI_596C07 (AT genome) | |
| **5** | ATTTTGCCGATTTCGGAAC | Genotyping of *avp2;2-1* | ~289 bp |
| **765** | CAGAGAAAGATAGGAGCCATGA | SALK_044701 (T-DNA LB) | |
| **764** | GGCTATAATATCACCCATTGCAG | Genotyping of *avp2;2-1* | 560 bp |
| **765** | CAGAGAAAGATAGGAGCCATGA | SALK_044701 (AT genome) | |
| **991** | TGAGCCAGCAGGTATGAGTC | Genotyping of *avp2;2-2* | ~650 bp |
| **5** | ATTTTGCCGATTTCGGAAC | SALK_138132 (T-DNA LB) | |
| **991** | TGAGCCAGCAGGTATGAGTC | Genotyping of *avp2;2-2* | 866 bp |
| **992** | CGCAAACATTAGCATTGCAGC | SALK_138132 (AT genome) | |

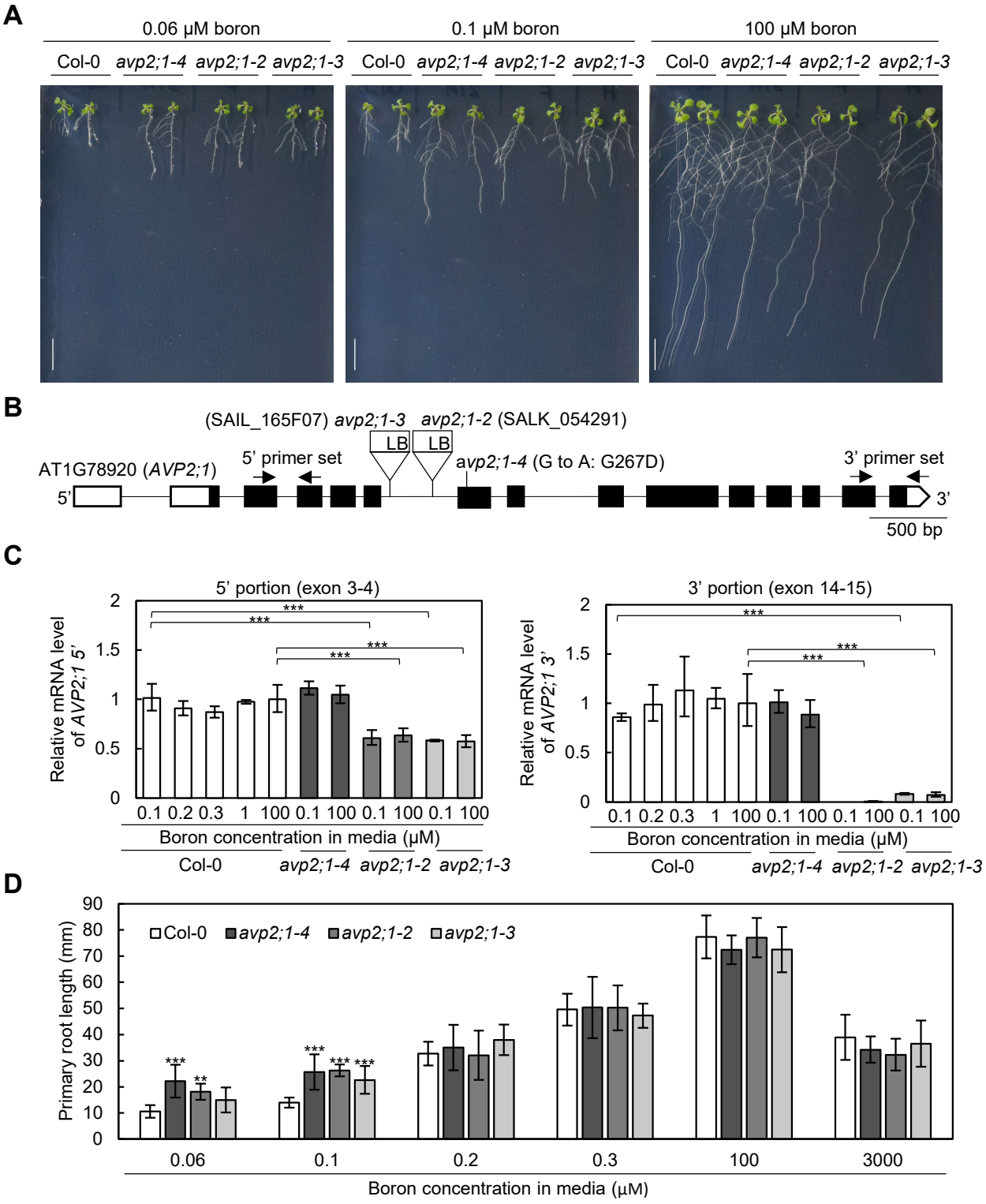


**Figure 1.** Growth analysis and mRNA level in wildtype Col-0 and *avp2;1* mutants. **(A)** Photos of plants under 0.06 µM (very low), 0.1 µM (low) and 100 µM (normal) boron conditions. (scale bar: 10 mm). **(B)** *AVP2;1* gene structure showing the point mutation, T-DNA insertion positions and primer positions used for mRNA quantification. White and black boxes indicates UTRs and coding regions while the connecting black line indicates the intron. **(C)** mRNA quantification of *AVP2;1* in roots of wildtype Col-0 and *avp2;1* mutants using primers at the 5' portion and 3' portion respectively under various concentrations of boron. *EF1α* was used for normalization. Means ± SD are shown (n=3-4). Statistical analysis was not performed for *avp2;1-2* under 0.1 µM at the 3' portion because it was below detection limit. **(D)** Primary root length of wildtype Col-0 and *avp2;1* mutant lines under various boron concentrations. Means ± SD are shown (n=6-11). All the analysis in Fig 1 were done using 9-d-old plants grown in solid media. ***$P < 0.001$,**$P < 0.01$, compared with wildtype Col-0 under the same boron conditions (Dunnett's test)

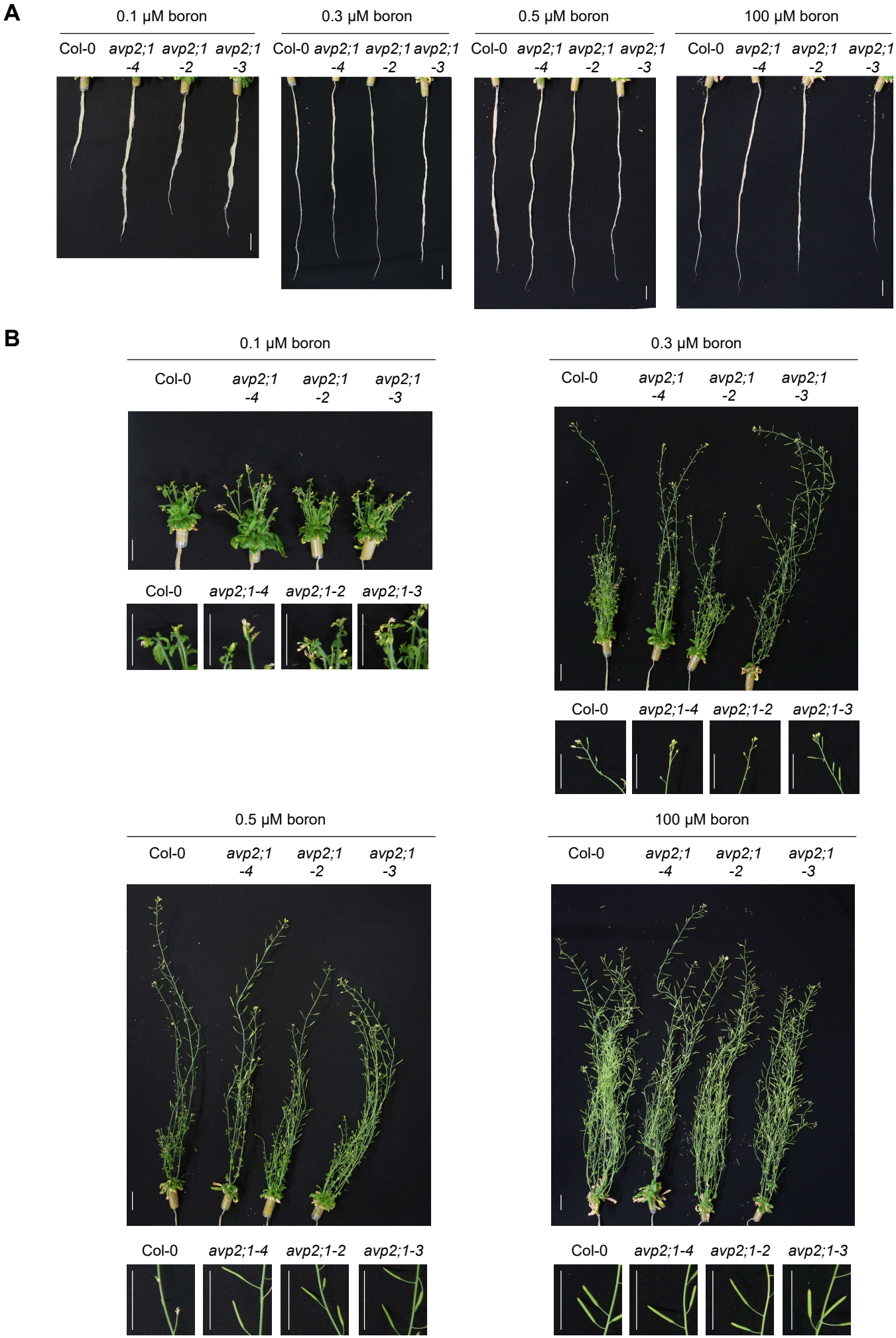


**Figure 2.** Fertility test in wildtype Col-0 and *avp2;1* mutants. **(A)** Roots of 56-d-old wildtype Col-0 and *avp2;1* mutants grown hydroponically under 0.1 µM (low), 0.3 µM, 0.5 µM (mildly low) and 100 µM (normal) boron conditions. (scale bar: 20 mm). **(B)** Aerial parts of wildtype Col-0 and *avp2;1* mutants grown under same conditions as (A). (scale bar: 20 mm).

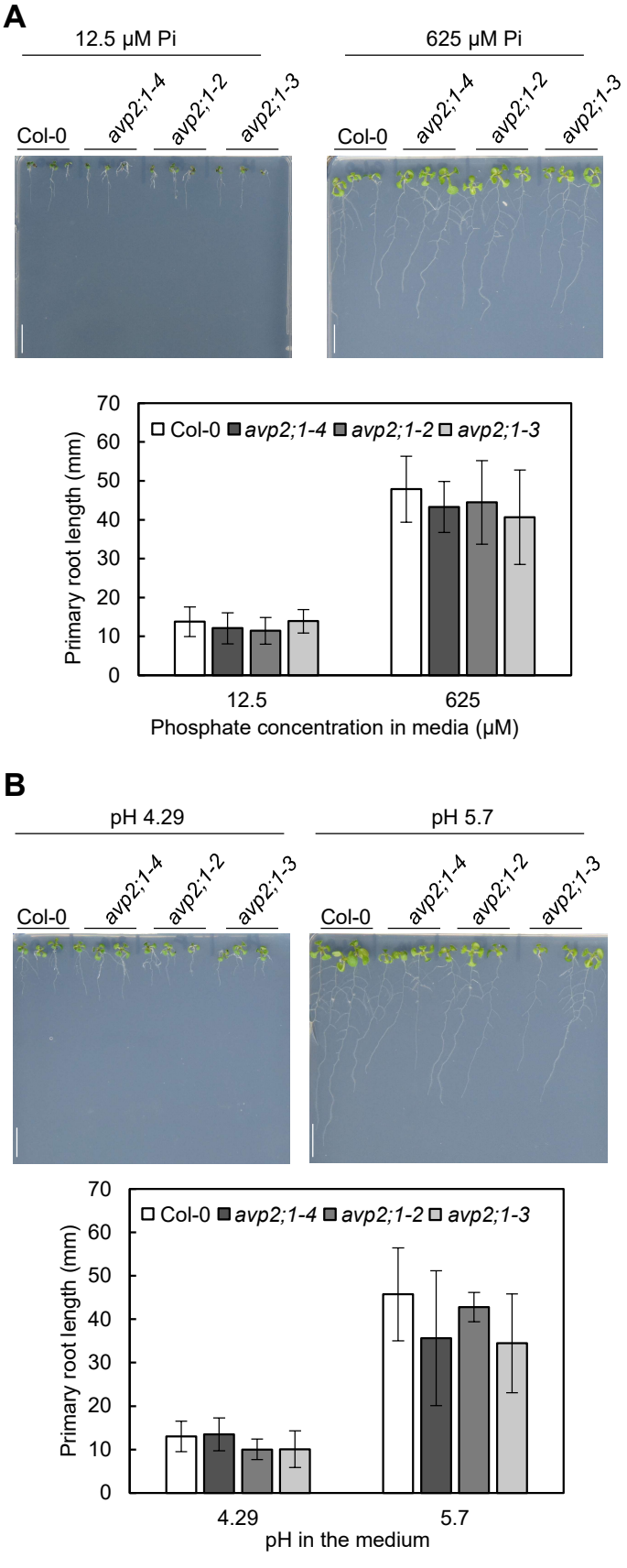


**Figure 3.** Growth test of wildtype Col-0 and *avp2;1* mutants under low phosphorus and low pH conditions. **(A), (B)** Primary root of wildtype Col-0 and *avp2;1* mutants under low (12.5 µM) and normal (625 µM) phosphate conditions (A) and low pH (4.29) and normal pH (5.7) conditions (B). (Scale bar: 10 mm). All growth test was performed using 9-d-old plants grown in solid media. Mean ±SDs are shown (n=13-27). $P > 0.05$ compared with wildtype Col-0 under the same phosphorus and pH conditions (Dunnett's test)

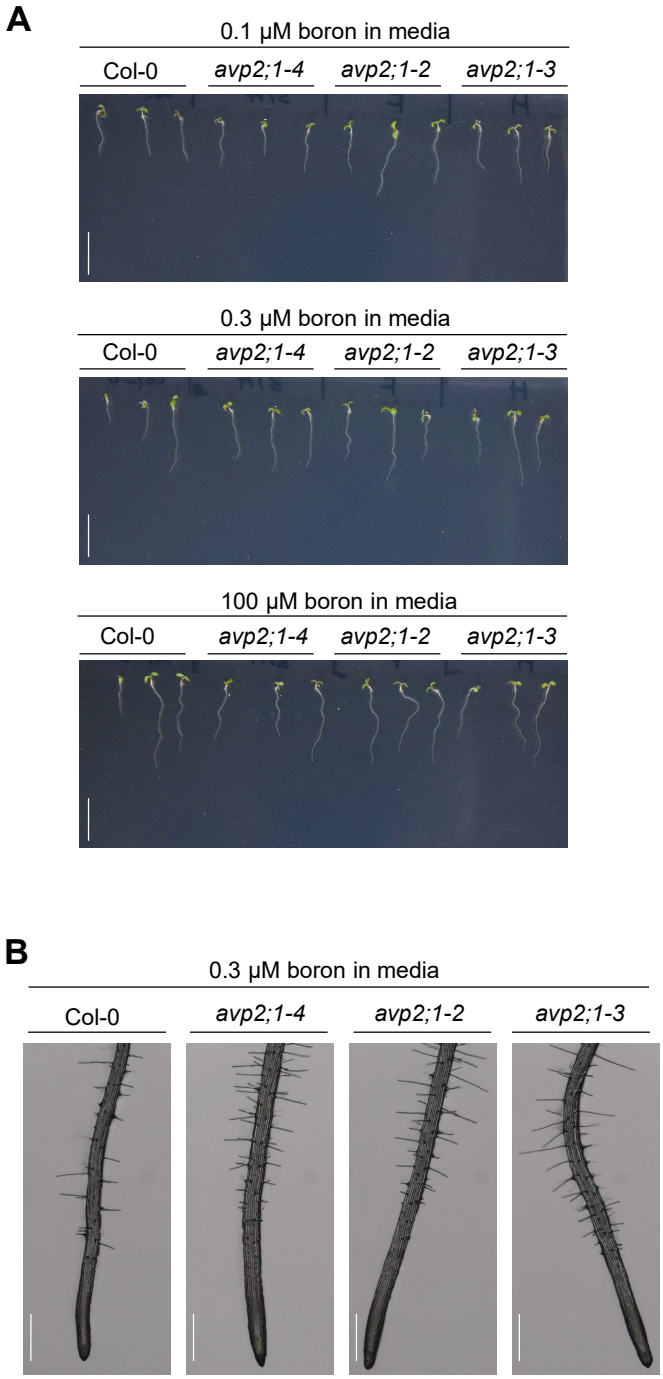


**Figure 4.** Observation of the root cells of wildtype Col-0 and *avp2;1* mutants. **(A)** Images of wildtype Col-0 and *avp2;1* mutant lines grown under low (0.1 µM), mildly low (0.3 µM) and normal (100 µM) boron conditions in solid media for root cell observation. (Scale bar: 10 mm). **(B)** Stereomicroscopic images of wildtype Col-0 and *avp2;1* mutants root tips under mildly low (0.3 µM) boron conditions (scale bar: 400 µm). Plants were grown for 5 days for this analysis.

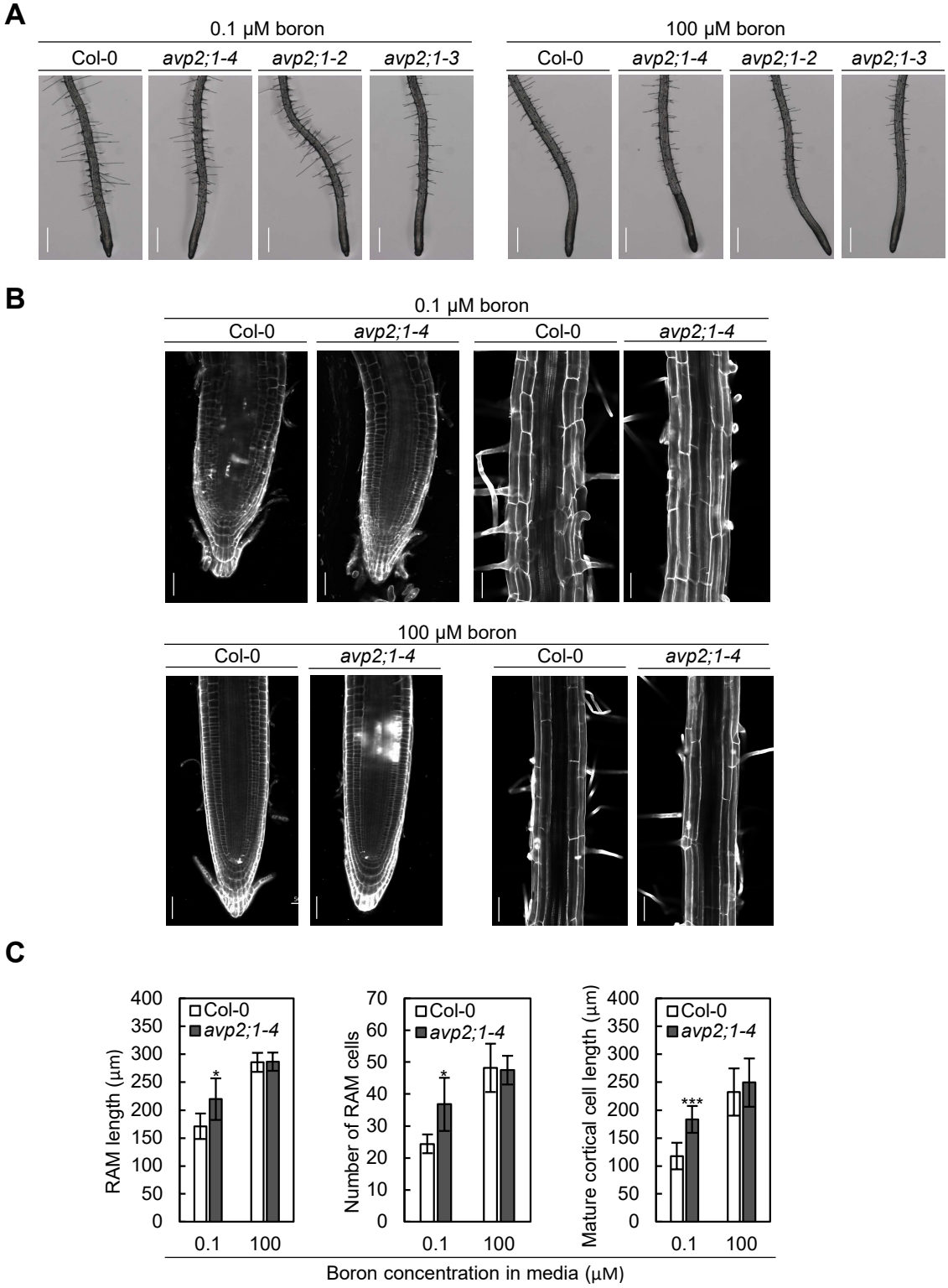


**Figure 5.** Observation of the root cells of Col-0 and *avp2;1* mutants. **(A)** Stereomicroscopic images of root tips of wildtype Col-0 and *avp2;1* mutants grown under low (0.1 µM) and normal (100 µM) boron conditions. (scale bar: 400 µm). **(B)** Confocal images of roots of wildtype Col-0 and *avp2;1-4* grown under low (0.1 µM) and normal (100 µM) boron conditions showing its meristematic zone and mature zone. (scale bar: 50 µm). **(C)** Root apical meristem (RAM) length (n=5-7 plants), number of RAM cells (n=5-7 plants), and mature cortical cell length (n=5-7 plants, means of 2-12 cells per plant were taken) of wildtype Col-0 and *avp2;1-4* under 0.1 µM and 100 µM boron conditions. Means ± SD are shown. All the analysis in Figure 2 were done using 5-d-old plants grown in solid media. ***$P < 0.001$,*$P < 0.05$, compared with wildtype Col-0 under the same boron conditions (Student's t-test)

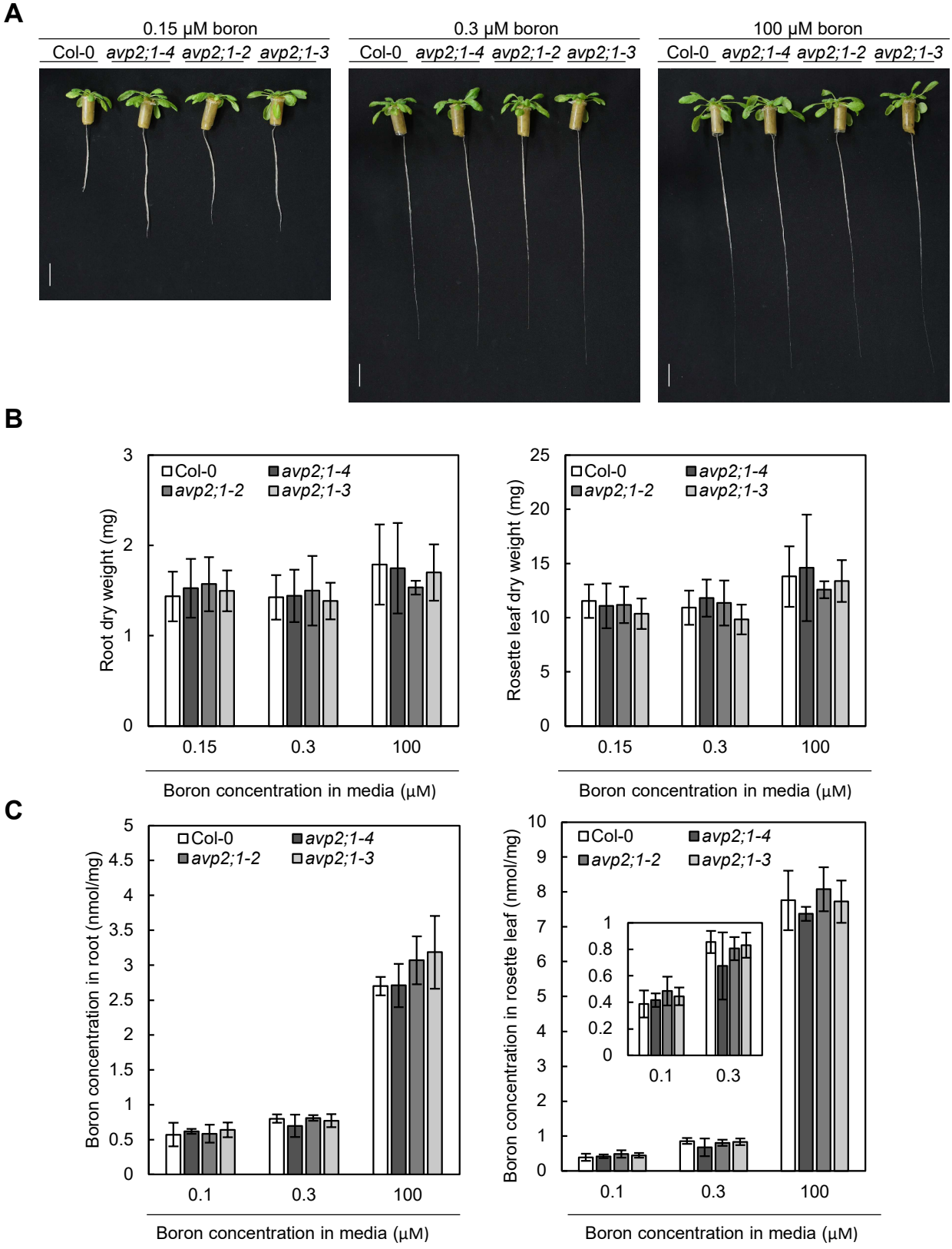


**Figure 6.** Growth in hydroponic culture and boron concentration in root and rosette leaves. **(A)** Representatives of wildtype Col-0 and *avp2;1* mutants grown in a hydroponic culture under low (0.15 µM), mildly low (0.3 µM) and normal (100 µM) boron conditions for 35 days. (scale bar: 20 mm). **(B)** Dry weight of wildtype Col-0 and mutant roots and rosette leaves grown under the same condition as (A). **(C)** Boron concentration in root and rosette leaves of wildtype Col-0 and *avp2;1* mutants grown for 42 days under low (0.1 µM, the B concentration in media was increased to 0.15 µM after 19 days of culture in liquid MGRL media), mildly low (0.3 µM) and normal (100 µM) boron conditions using hydroponic culture. Means ± SD are shown (n=5-6). $P > 0.05$, compared with wildtype Col-0 under the same boron conditions (Dunnett's test)

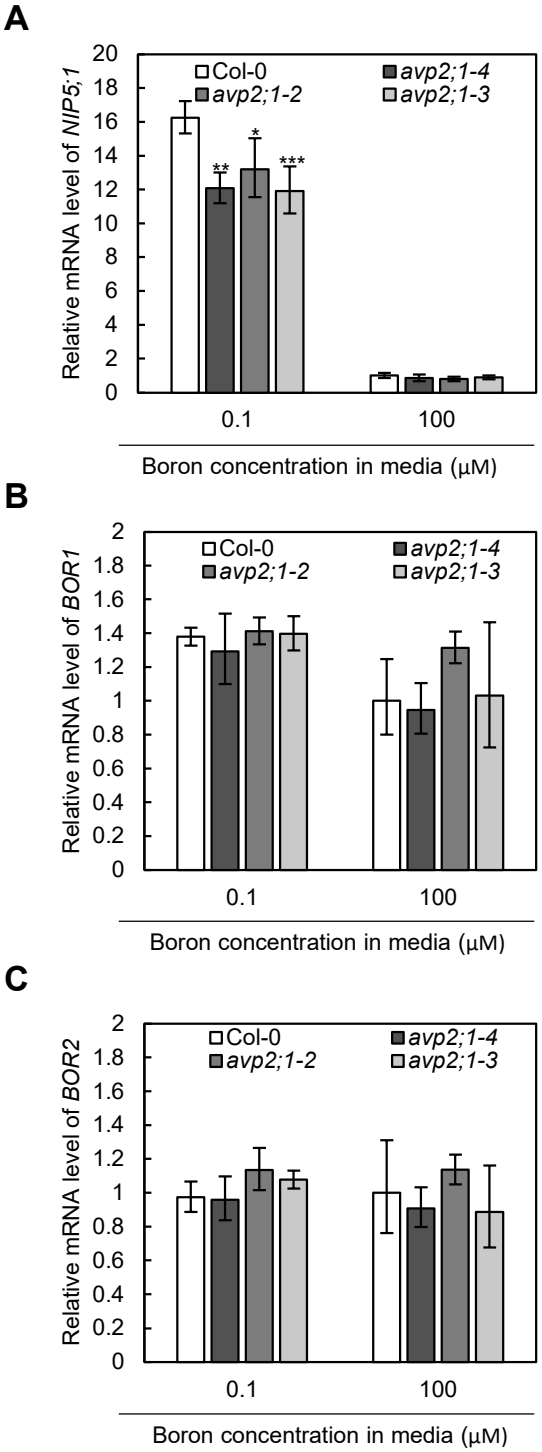


**Figure 7.** mRNA levels of boron transporter genes. **(A),(B),(C)** Relative mRNA quantification of *NIP5;1* (A) *BOR1* (B) and *BOR2* (C) in root of wildtype Col-0 and *avp2;1* mutant lines under low (0.1 μM) and normal (100 μM) boron condition. mRNA extracted from 9-d-old plants grown in solid media were used for all analysis. *EF1α* was used for normalization. The data was standardized by the value of Col-0 under normal (100 μM) boron condition which was set as 1. Means ± SD are shown (n=3-4). ***$P < 0.001$, **$P < 0.01$, *$P < 0.05$ compared with wildtype Col-0 under the same boron conditions (Dunnett's test)

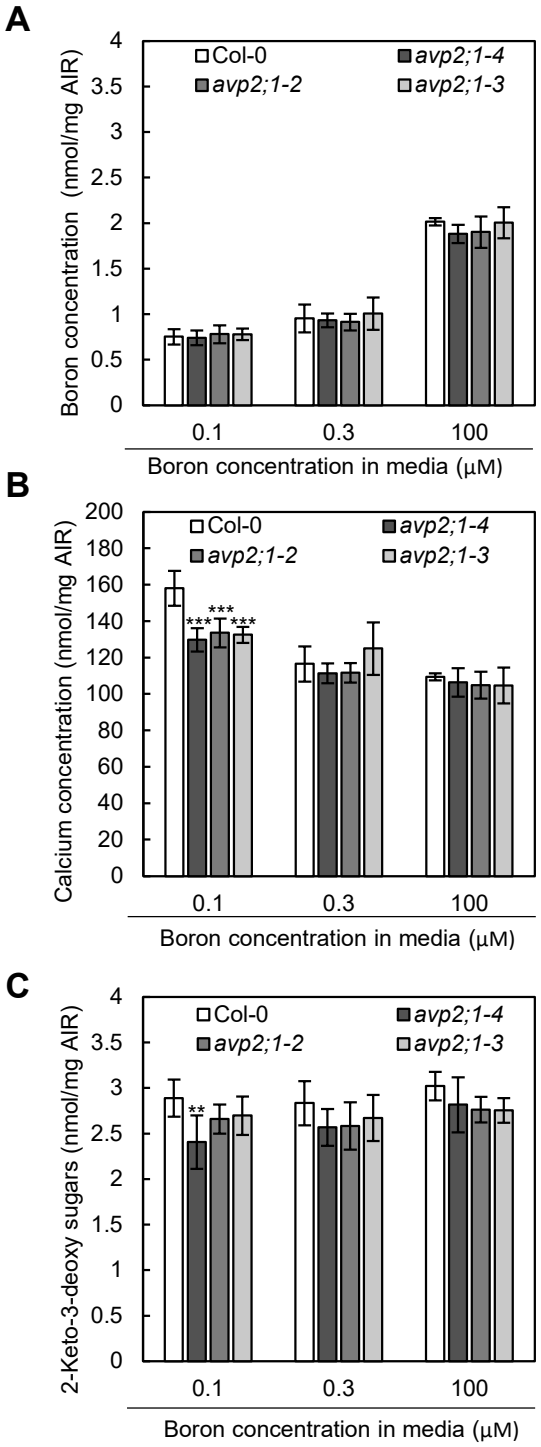


**Figure 8.** Boron, calcium and RG-II specific sugars in root cell wall extracted as alcohol insoluble residue (AIR). **(A),(B),(C)** Concentration of boron (A) calcium (B) and RG-II specific sugar, 2-keto-3-deoxy sugars (C) in root AIR of wildtype Col-0 and *avp2;1* mutants. The same AIR extracted from 9-d-old plants grown under low (0.1 µM), mildly low (0.3 µM) and normal (100 µM) boron conditions in solid media were used for all analysis. Means ± SD are shown (n=4-6). ***$P < 0.001$, **$P < 0.01$ compared with wildtype Col-0 under the same boron conditions (Dunnett's test)

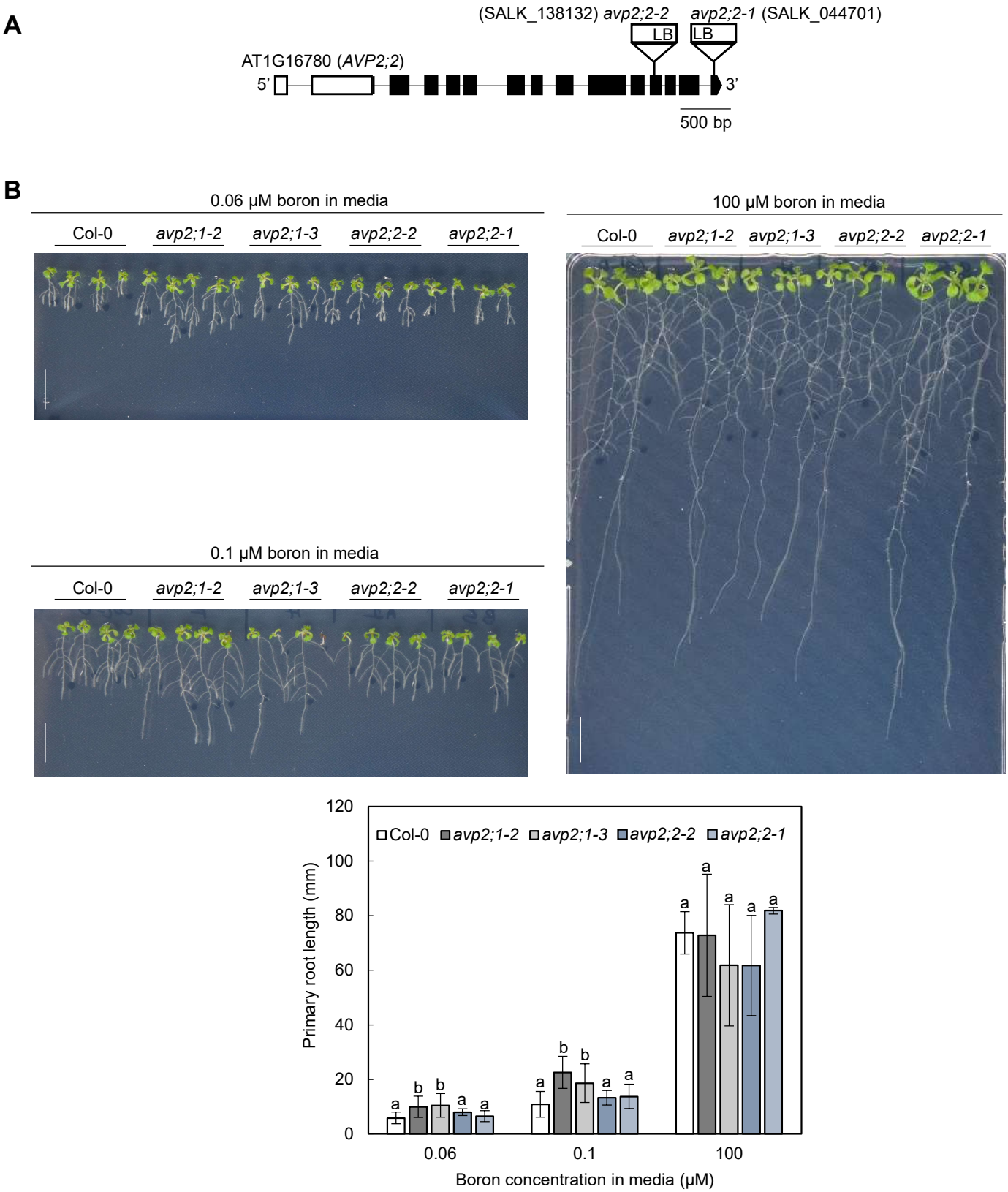


**Figure 9.** Growth analysis of wildtype Col-0 and *avp2;2* mutants under various boron concentrations. **(A)** Gene structure of *AVP2;2* (AT1G16780) showing insertion positions of T-DNA. **(B)** Primary root length of wildtype Col-0, *avp2;1* and *avp2;2* mutants plant lines grown under very low (0.06 μM), low (0.1 μM) and normal (100 μM) boron conditions. (Scale bar=10 mm). *avp2;2-2* and *avp2;2-1* are SALK_138132 and SALK_044701 lines, respectively. Plants used for analysis are 11-d-old. Mean ±SDs are shown (n=15-27). Different alphabets indicate significant differences among plants. $P < 0.001$ (Tukey-Kramer test)

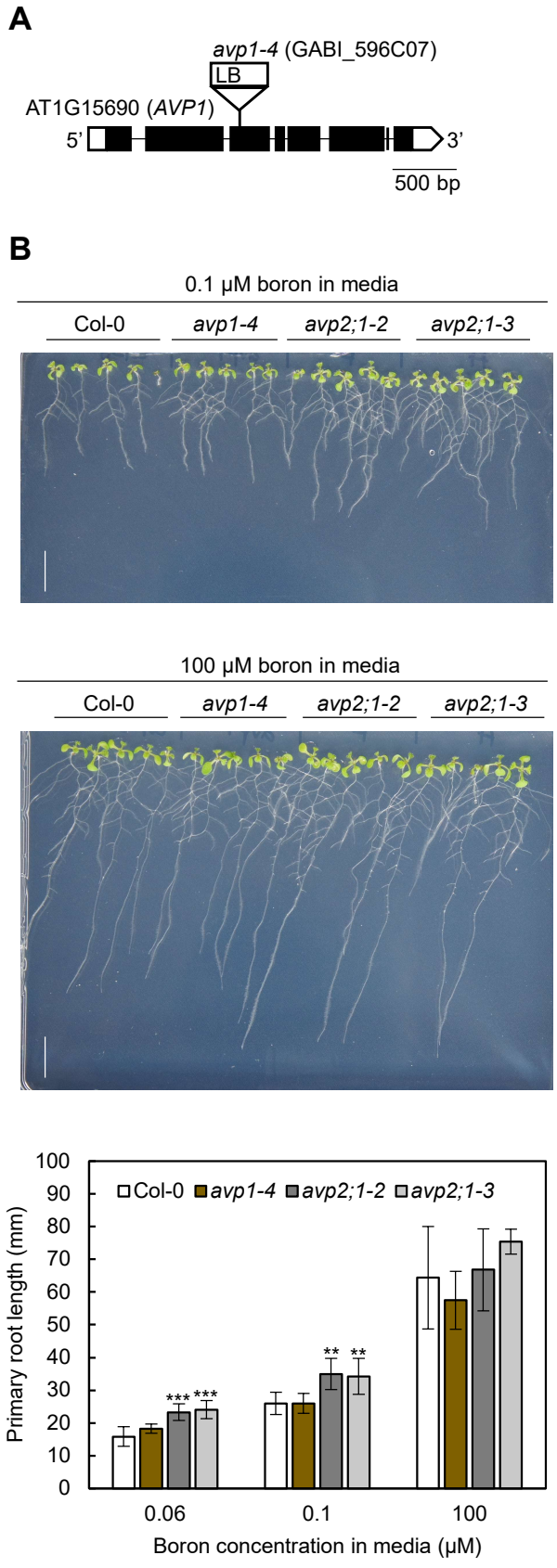


**Figure 10.** Growth test of wildtype Col-0, *avp1* mutant line and *avp2;1* T-DNA lines under low and normal boron conditions. **(A)** Gene structure of *AVP1* (AT1G15690) showing insertion position of T-DNA. **(B)** Col-0, a*vp1-4, avp2;1-2* and *avp2;1-3* primary root length under very low (0.06 µM), low (0.1 µM) and normal (100 µM) boron conditions. (Scale bar: 10 mm). Plants were grown for 9 days. Mean ±SDs are shown (n=6-13). ***$P$ < 0.001,**$P$ < 0.01, compared with wildtype Col-0 under the same boron conditions (Dunnett's test)

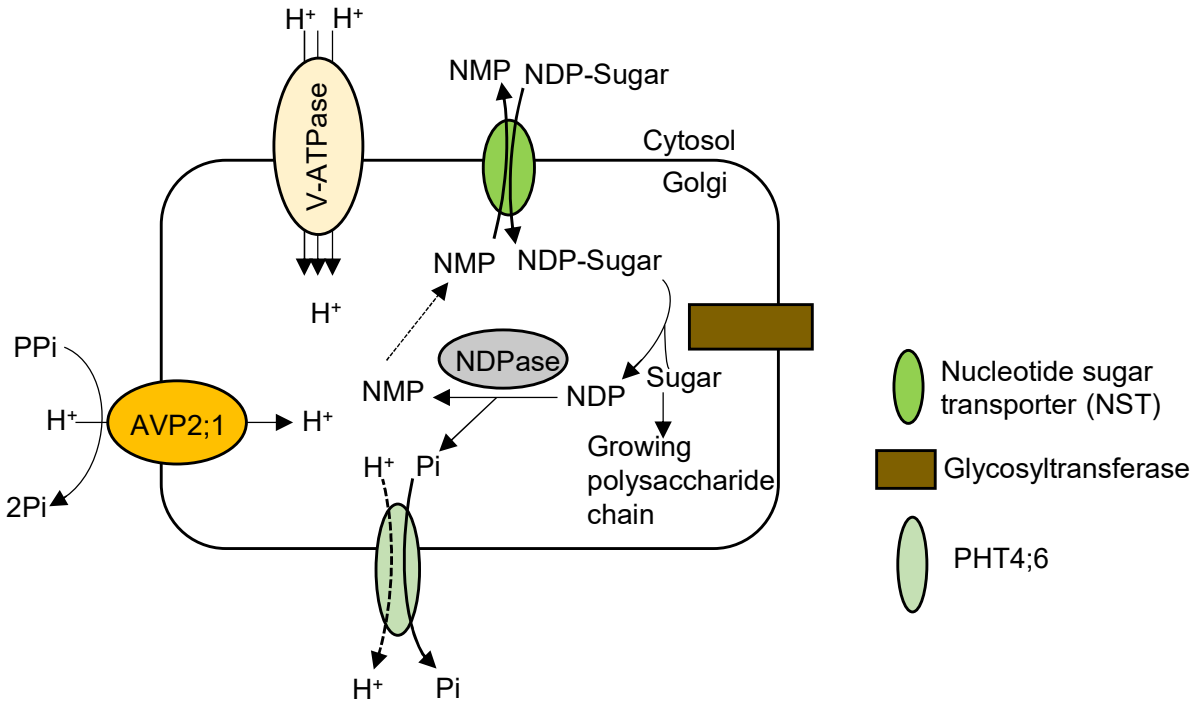


**Figure 11.** Model of pectin synthesis and the contribution of AVP2;1 to the maintenance of ion homeostasis in the Golgi apparatus. By the activity of the nucleotide sugar transporter (NST) which is an NDP-sugar/NMP antiporter, nucleoside di-phosphate sugar (NDP-sugar) is imported from the cytosol into the Golgi lumen. The sugar moiety is then transferred to a growing chain of polysaccharide via the action of glycosyltransferase and the resulting NDP is hydrolyzed by NDPase to nucleoside monophosphate (NMP) and inorganic phosphate. The NMP concentration gradient drives transport of NDP-sugar via NSTs as NDP-sugar/NMP antiporters. The inorganic phosphate released from NDP hydrolysis is exported into the cytosol from Golgi apparatus via a phosphate transporter (PHT4;6). AVP2;1 helps to maintain ionic homeostasis and acidic state of the Golgi apparatus via its proton pumping activity thereby enhancing the process of pectic polysaccharide synthesis.